

69-19
Copy 1

WOODS HOLE OCEANOGRAPHIC INSTITUTION

REFERENCE NO. 69-19

DEEP-SEA COREHEAD CAMERA PHOTOGRAPHY
AND PISTON CORING

by

F. W. McCoy, Jr., R. P. Von Herzen,
D. M. Owen and P. R. Boutin

*This document has been approved for public
release and sale; its distribution is unlimited.*

WOODS HOLE, MASSACHUSETTS

WOODS HOLE OCEANOGRAPHIC INSTITUTION
Woods Hole, Massachusetts

REFERENCE NO. 69-19

DEEP-SEA COREHEAD CAMERA PHOTOGRAPHY
AND PISTON CORING

by

F. W. McCoy, Jr., R. P. Von Herzen,
D. M. Owen and P. R. Boutin

March 1969

TECHNICAL REPORT

*Partially supported by National Science
Foundation Grants GA-1077 and GA-1209 and
submitted to the Office of Naval Research
under Contract Nonr-4029(00); NR 260-101,
and N00014-66-C0241; NR 083-004.*

*Reproduction in whole or in part is permitted
for any purpose of the United States Government.
In citing this manuscript in a bibliography, the
reference should be followed by the phrase:
UNPUBLISHED MANUSCRIPT.*

*This document has been approved for public
release and sale; its distribution is unlimited.*

Approved for Distribution

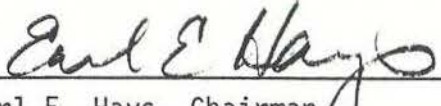

Earl E. Hays, Chairman
Department of Geology and Geophysics



TABLE OF CONTENTS

	<u>Page No.</u>
ABSTRACT	i
I. INTRODUCTION	1
II. DESCRIPTION OF THE EQUIPMENT	6
Cameras and Strobe-Light Source	6
Coring Apparatus.	9
Corer Design	11
Shipboard Operation	14
III. OPERATION OF THE PISTON CORER	16
Introduction	16
Descent	16
Tripping and Free-Fall	18
Penetration	22
Motion While in Bottom	34
Pull-Out.	37
Ascent	37
Summary	39
IV. PENETRATION, CORE SHORTENING AND CORE DISTURBANCES	41
Introduction	41
Measurement of Penetration.	43
Immobilization of the Piston.	43
Relationship Between the Core Recovered and Penetration	52
Comparison of Pilot Cores and Piston Cores	54
Core Shortening	54
Relationship Between the Mud-Mark and Penetration	55
Relationship Between the Geothermal Gradient and Penetration	55
Relationship Between the Vertical Deviation of the Corer in the Bottom and Penetration	58
Relationship Between Stratigraphic Dips in the Cores and the Vertical Deviation of the Corer in the Bottom	58
Summary	59

TABLE OF CONTENTS (Continued)

- 2 -

	<u>Page No.</u>
V. BOTTOM CURRENT MEASUREMENTS.	60
VI. RECOMMENDATIONS FOR FUTURE PISTON CORING	64
REFERENCES	66

LIST OF FIGURES AND PLATES

		Page No.
Figure 1.	Ship's track and coring stations - CHAIN cruise 75.	3
Figure 2.	Piston corer and instrumentation prior to lowering	7
Figure 3.	Exterior electrical connections between cameras and light source	8
Figure 4.	Specifications of the corehead and core barrels	10
Figure 5.	Positioning of the bracket arm beneath the corehead.	12
Figure 6.	Wind direction and average azimuth of the tripping arm during descent on 33 coring stations.	17
Figure 7.	Deviation of tripping arm azimuth from wind direction and presumed ship's drift during 12 coring stations.	19
Figure 8.	Time for free-fall as a function of the height of free-fall	21
Figure 9.	Penetration of the piston corer into the bottom on station 2	23
Figure 10.	Penetration of the piston corer into the bottom on station 17.	24
Figure 11.	Penetration of the piston corer into the bottom on station 31	25
Figure 12.	Approximate time for complete corer penetration as a function of the height of free-fall	27
Figure 13.	Small manganese nodules near the core barrel on station 2.	29
Figure 14.	Portion of sediment mound surrounding core barrel on station 37	31
Figure 15.	Portion of sediment mound surrounding core barrel on station 46	31
Figure 16.	Small channel cut through sediment mound near core barrel on station 17	32
Figure 17.	Depression surrounding the core barrel on station 7	32
Figure 18.	Pilot corer and piston corer in the bottom during station 14.	33
Figure 19.	Bending of the piston corer on station 10	35

LIST OF FIGURES AND PLATES (Continued)

- 2 -

Page No.

Figure 20.	Calculated maximum stress for vertical deviations of 6°, 12° and 24° for varying lengths of core barrel protruding above the bottom	36
Figure 21.	Pilot corer resting on its side near the piston corer on station 18	38
Figure 22.	Winch cable wrapped around the piston corer during station 4, ATLANTIS II cruise 42	38
Figure 23.	Calibration photograph used to determine the ratio of the bracket arm shadow width to the width of the bracket arm with penetration to within 8 ft of the base of the corehead	45
Figure 24.	Calibration curve for determining amount of penetration for the camera focused at 1.8 m (6 ft).	46
Figure 25.	Calibration curve for determining amount of penetration for the camera focused at 4.9 m (16 ft)	47
Figure 26.	Amount of cable elongation as a function of the length of cable out.	49
Figure 27.	Extra cable necessary due to elastic rebound as a function of the time for free-fall	51
Figure 28.	Relationship between the photographically measured penetration and the length of core recovered	53
Figure 29.	Relationship between the position of the exterior mudmark and the photographically measured penetration	56
Figure 30.	Relationship between the implied penetration as extrapolated from the thermal gradient (TG) and the photographically measured penetration.	57
Figure 31.	Bottom currents producing a narrow streaming sediment cloud around the base of the core barrel during station 16	61
Figure 32.	Higher, diffuse sediment cloud during station 44 moving in response to bottom currents.	61
Figure 33.	Bottom current directions between the Lesser Antilles and the Mid-Atlantic Ridge	63
Plate I.	Sequence of photographs taken by both cameras during coring operations on station 7	69

LIST OF TABLES

	Page No.
Table I. Locations, Depths, and Photographic Results of CHAIN 75 Coring Stations	4
Table II. Corehead camera aperture settings	9
Table III. Hvorslev's Ratios of the Piston Corer	13
Table IV. Penetration, Length of Cores, Core Shortening, and Corer Orientations and Vertical Deviation in Bottom	44

ABSTRACT

Cameras were mounted in a newly designed corehead of a piston corer and used to photograph coring operations during 36 stations on CHAIN cruise 75 and 28 stations on ATLANTIS II cruise 42. Through the analysis of these photographs, the deep-water operation of a piston corer during its descent, tripping, impact with the bottom, and ascent has been studied, providing information on the corer's stability, effectiveness in obtaining a bottom sample, and influence on the nearby sea-floor. Accurate determinations of the amount of penetration were possible, allowing comparisons to be made with the more indirect methods of determining penetration and with the length of core recovered. Sediment clouds produced by bottom currents were noticed in many of the bottom photographs. A number of suggestions are made for future piston coring operations.

The corer descends with little rotation and swinging. Free-fall and penetration generally take place in less than 5 seconds, with a rotation of 20-60° and an increase of about 6° in vertical deviation. During penetration, the corer disturbs the surrounding sea floor, producing both mounds and depressions around the core barrels. While resting in the bottom, the corer is very stable although some wobbling does occur. Considerable rotation takes place during both pull-out and ascent; frequent sediment discharges from the piston corer occur.

No consistent relationship was found between the amount of penetration and the length of core recovered, and thus with the degree of core shortening. Comparisons between piston and pilot cores indicate that the piston cores have been shortened and disturbed relative to the pilot cores, and that as much as a meter of the upper portion of the piston core has been lost. The position of the mud-mark appears to be a reliable indicator of the amount of penetration; estimates by extrapolation of the thermal gradient to the surface are less reliable. The vertical deviation of the corer in the bottom does not influence the amount of penetration. Stratigraphic dips in the recovered cores correspond poorly to this vertical deviation in the bottom.

I. INTRODUCTION

The piston corer was developed in an attempt to improve upon the smaller gravity corers that were then being used (Kullenberg, 1947). By incorporating a piston that remained attached to the lowering cable and was adjusted to rest at the sediment surface, frictional forces within the core barrel were greatly reduced as the corer penetrated the bottom sediment. Higher impact velocities were achieved by letting the piston corer free-fall from predetermined distances above the bottom. The intention of this new design was to significantly increase the amount of penetration and decrease any disturbances to the core. Yet serious deformation and disturbances do occur in piston cores because of incomplete penetration or improper adjustment of the piston. Frequently, for example, the upper portion of a piston core may be lost; thus it has now become a common practice to use a small gravity corer both to initiate free-fall and as a sampling device to retain the surface sediment. Despite excellent theoretical treatments (Kullenberg, 1947, 1955), piston coring has been hampered by a lack of understanding about the operation and behavior of the corer in deep water during the coring process.

Photographic techniques can be used to study the in situ operation and behavior of a piston corer in deep water. By placing a compass and inclinometer within the field of view of a camera, the orientation and vertical deviation of the corer in the bottom can be determined, allowing cores to be oriented for paleomagnetic studies and the direction of bottom currents to be determined where they exist. Photographs show the amount of penetration by the piston corer into the bottom, from which comparisons can be made with the length of core recovered, and provide a visual record of the sea floor at each coring station.

Corehead cameras were first used and described by Ewing, Hayes and Thorndike (1967) using one camera and a 12 second time lapse between pictures. A modified version was designed at the Woods Hole Oceanographic Institution using two cameras and a 5 second time lapse between pictures. This modified design was used successfully with a piston corer during CHAIN cruise 75, where photographs were obtained on 35 out of 36 coring stations, resulting in over 19,000 photographs taken while the corer was descending, resting in the bottom, and ascending. With the exception of one coring station on the Outer Ridge

north of Puerto Rico and one coring station in the Caribbean, all coring stations were made during November and December, 1967, along two traverses between Barbados and the Mid-Atlantic Ridge, and in the Barracuda Fault Zone area. The track plot and approximate coring station positions are shown in figure 1; Table I summarizes the photographic results from each station.

This report is concerned with the description of the equipment and the interpretation of the photographs as they pertain to the operation of the piston corer. The relationship between the retrieved cores and the photographically measured penetration and vertical deviation of the piston corer in the bottom, the exterior mud mark along the core barrels, the implied penetration of the corer from heat-flow data, and to the interpretation of sediment structures within the cores, are also discussed. Bottom current information obtained from the photographs has been reported elsewhere (McCoy, 1969), and is briefly summarized. These corehead camera photographs, and all interpretations of them, describe only the operation and characteristics of the particular piston corer used during CHAIN cruise 75; in general, however, these interpretations should be applicable to other piston coring apparatus and techniques. Additional brief comments are made from corehead camera photographs taken on 28 coring stations during ATLANTIS II cruise 42 (July, 1968).

It is extremely difficult to acknowledge all those who have significantly contributed to the final preparation of this report, especially since the original design and techniques of operating the piston corer are the product of many years of experience and development by numerous members of the Woods Hole Oceanographic Institution. Discussions with R. L. Chase, F. B. Wooding, K. O. Emery, D. A. Ross, C. D. Hollister, and R. T. Nowak have been most beneficial. An earlier version of the manuscript was reviewed by K. O. Emery and D. A. Ross. Our thanks to C. Ronne for printing many of the pictures, also to J. F. Jones for core photography and other assistance. The work at sea was made possible only by the extremely cooperative efforts of the officers and crew of the R. V. CHAIN, and the scientists on board the ship during the cruise. CHAIN cruise 75 was supported by the National Science Foundation under grant GA-1209, and ATLANTIS II cruise 42 was funded by the Office of Naval Research under contract Nonr 241-9 and by the National Science Foundation under grant GA-1077. The preparation of this manuscript was supported by the Office of Naval Research under contract Nonr-4029(00).

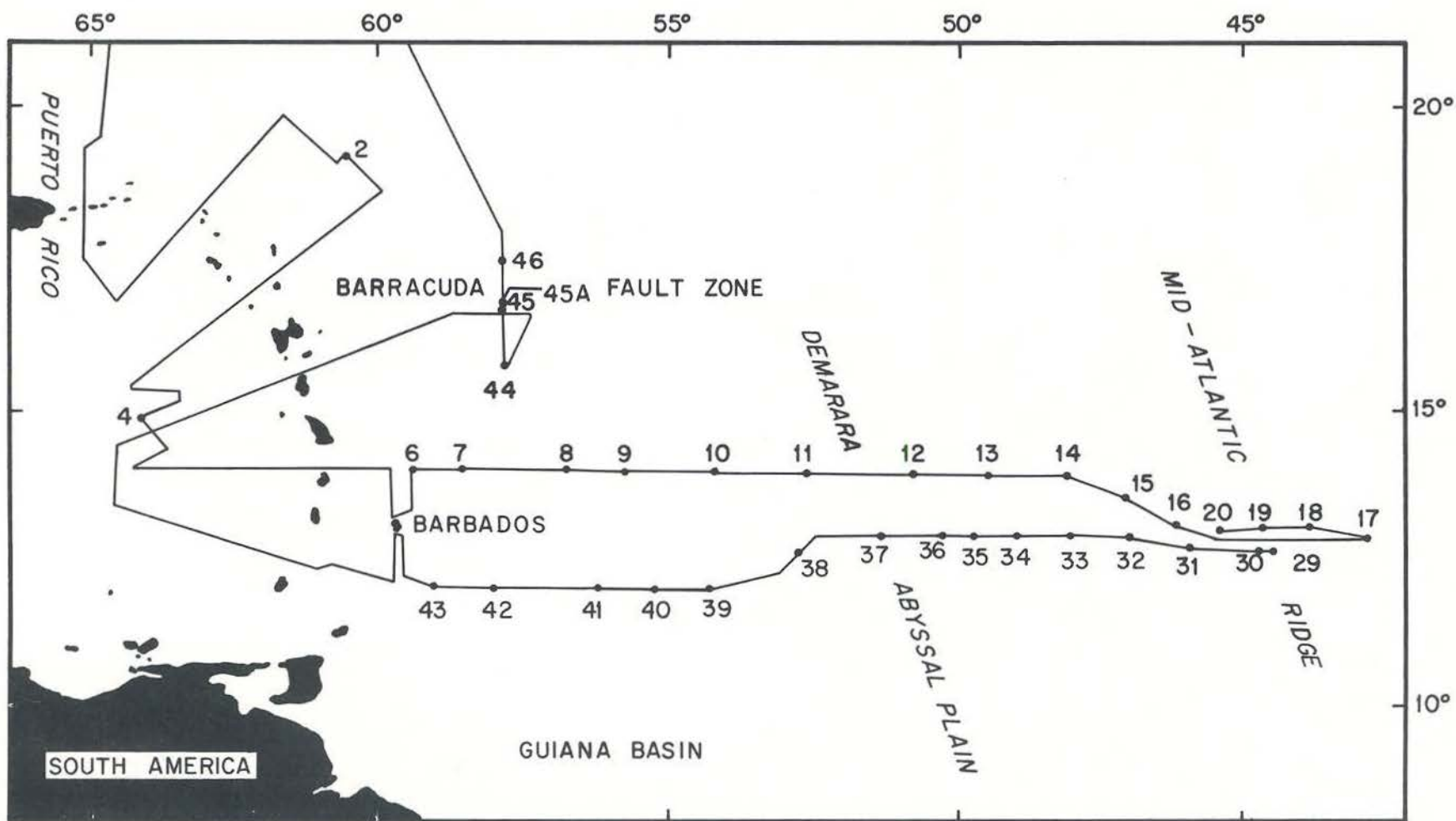


Figure 1. Ship's track during CHAIN cruise 75 with coring station positions and station numbers.

Table I

Locations, Depths, and Photographic Results of CHAIN 75 Coring Stations

Station No.	Latitude (°N)	Longitude (°W)	Depth (cor. m.)	Physiographic Location	Photographic Results
2	19°30'	60°47'	5259	outer ridge north of Puerto Rico	pictures throughout station
4	14°45'	63°59'	2385	Aves Ridge, Caribbean Sea	pictures during ascent only
6	14°17'	59°37'	3351	Lesser Antilles island arc	pictures throughout station
7	14°14'	58°25'	3540	eastern slopes of Lesser Antilles island arc	pictures throughout station
8	14°14'	55°38'	5175	Guiana Basin abyssal hills	pictures during ascent only
9	14°14'	55°49'	5143	Guiana Basin abyssal hills	no pictures
10	14°09'	54°07'	5349	Guiana Basin abyssal hills	pictures throughout station, corer bent
11	14°18'	52°37'	4412	Demerara Abyssal Plain	pictures throughout station
12	14°15'	50°51'	4776	abyssal hills along western flank of Mid-Atlantic Ridge	pictures throughout station, lenses buried in mud on bottom - no bottom photos
13	14°13'	49°10'	4460	abyssal hills along western flank of Mid-Atlantic Ridge	pictures throughout station, corer bent
14	14°19'	48°06'	3997	western flank of Mid-Atlantic Ridge	pictures throughout station
15	13°55'	47°02'	4348	western flank of Mid-Atlantic Ridge	pictures throughout station
16	13°22'	46°09'	3787	western flank of Mid-Atlantic Ridge	pictures throughout station
17	13°16'	42°50'	4421	eastern flank of Mid-Atlantic Ridge	pictures throughout station
18	13°23'	43°54'	4112	eastern flank of Mid-Atlantic Ridge	pictures throughout station
19	13°24'	44°39'	3142	crest of Mid-Atlantic Ridge	pictures during ascent only
20	13°22'	45°24'	3532	crest of Mid-Atlantic Ridge	pictures throughout station, lenses buried in mud on bottom 5 sec. after penetration
29	12°57'	44°32'	3266	crest of Mid-Atlantic Ridge	pictures throughout station, lenses buried in mud on bottom - no bottom photos
30	12°57'	44°46'	3483	crest of Mid-Atlantic Ridge	pictures throughout station, lenses buried in mud on bottom 5 sec. after penetration
31	12°00'	46°00'	3218	western flank of Mid-Atlantic Ridge	pictures throughout station
32	13°05'	46°54'	3313	western flank of Mid-Atlantic Ridge	pictures throughout station
33	13°04'	47°59'	4068	western flank of Mid-Atlantic Ridge	pictures throughout station, manganese pavement (?) encountered
34	13°02'	48°52'	4705	abyssal hills along western flank of Mid-Atlantic Ridge	pictures throughout station, lenses buried in mud on bottom - no bottom photos

Table I (continued)

<u>Station No.</u>	<u>Latitude (°N)</u>	<u>Longitude (°W)</u>	<u>Depth (cor. m.)</u>	<u>Physiographic Location</u>	<u>Photographic Results</u>
35	13°04'	49°46'	4969	abyssal hills along western flank of Mid-Atlantic Ridge	pictures throughout station, lenses buried in mud on bottom 15 sec. after penetration
36	13°03'	50°47'	4818	abyssal hills along western flank of Mid-Atlantic Ridge	pictures throughout station, lenses buried in mud on bottom
37	13°06'	51°19'	5006	Demerara Abyssal Plain	pictures throughout station
38	12°49'	52°46'	5111	Guiana Basin abyssal hills	pictures throughout station
39	12°15'	54°15'	4684	Guiana Basin abyssal hills	pictures throughout station, lenses buried in mud on bottom - no bottom photos
40	12°10'	54°44'	4532	Guiana Basin abyssal hills	pictures throughout station, lenses buried in mud on bottom - no bottom photos
41	12°09'	56°49'	4443	Guiana Basin abyssal hills	pictures throughout station, lenses buried in mud on bottom - no bottom photos
42	12°03'	57°57'	2819	eastern slopes of Lesser Antilles island arc	pictures throughout station
43	12°11'	59°03'	2176	Lesser Antilles island arc	pictures throughout station
44	15°59'	57°44'	5434	abyssal plain south of Barracuda Fault Zone	pictures throughout station
45	16°51'	57°38'	5843	Barracuda Fault Zone	pictures throughout station, bottom faintly visible
45A	16°55'	57°38'	5843	Barracuda Fault Zone	pictures throughout station, bottom faintly visible
46	17°36'	57°43'	5546	abyssal plain north of Barracuda Fault Zone	pictures throughout station

II. DESCRIPTION OF THE EQUIPMENT

Cameras and Strobe-Light Source

The two cameras and strobe-light source were basically standard Edgerton, Germeschausen & Grier equipment, using 35 mm CA-9 and LS-9 systems (Edgerton, 1967). Their arrangement within the corehead is shown in figure 2. Due to space limitations within the corehead the equipment was modified to operate on 6 volts. Since the operations to be photographed would take place rather quickly, additional modifications were made in the cameras and light source to increase the framing rate to about 1 every 5 seconds. Instead of the customary 30.6 m (100 ft) rolls, 15.3 m (50 ft) lengths of film were exposed, resulting in approximately 22 minutes of operation at the increased flash rate.

In the strobe, a higher flash rate was obtained by substituting a 3-detent cam for the standard single-detent cam in the timing switch. Discharge capacitors rated at 240 microfarads were substituted in the flash unit, lowering the energy input to the flash to 50 watt-sec. This reduced light output proved to be sufficient.

The end of the film was used to terminate camera operation with a microswitch. Connections between the strobe and camera housings were made using the "synch" terminals, which, because of shutterless operation in the cameras, were not being used. The exterior connections are diagrammed in figure 3.

Lenses were standard Hopkins f/4.5 adjustable-aperture lenses, with an effective focal length (in air) of 35 mm (Hopkins and Edgerton, 1961). One camera was focussed on the compass and inclinometer mounted on the bracket arm at a distance of 1.8 m (6 ft), and the other at a distance of 4.9 m (16 ft) -- the anticipated maximum range at which clear photos would result with partial penetration of the corer. It was anticipated that one camera or the other would show the bottom in focus as it approached the core weight and the combined depths of fields would cover the entire range. The angular field of view for the cameras in water was 37° x 53°.

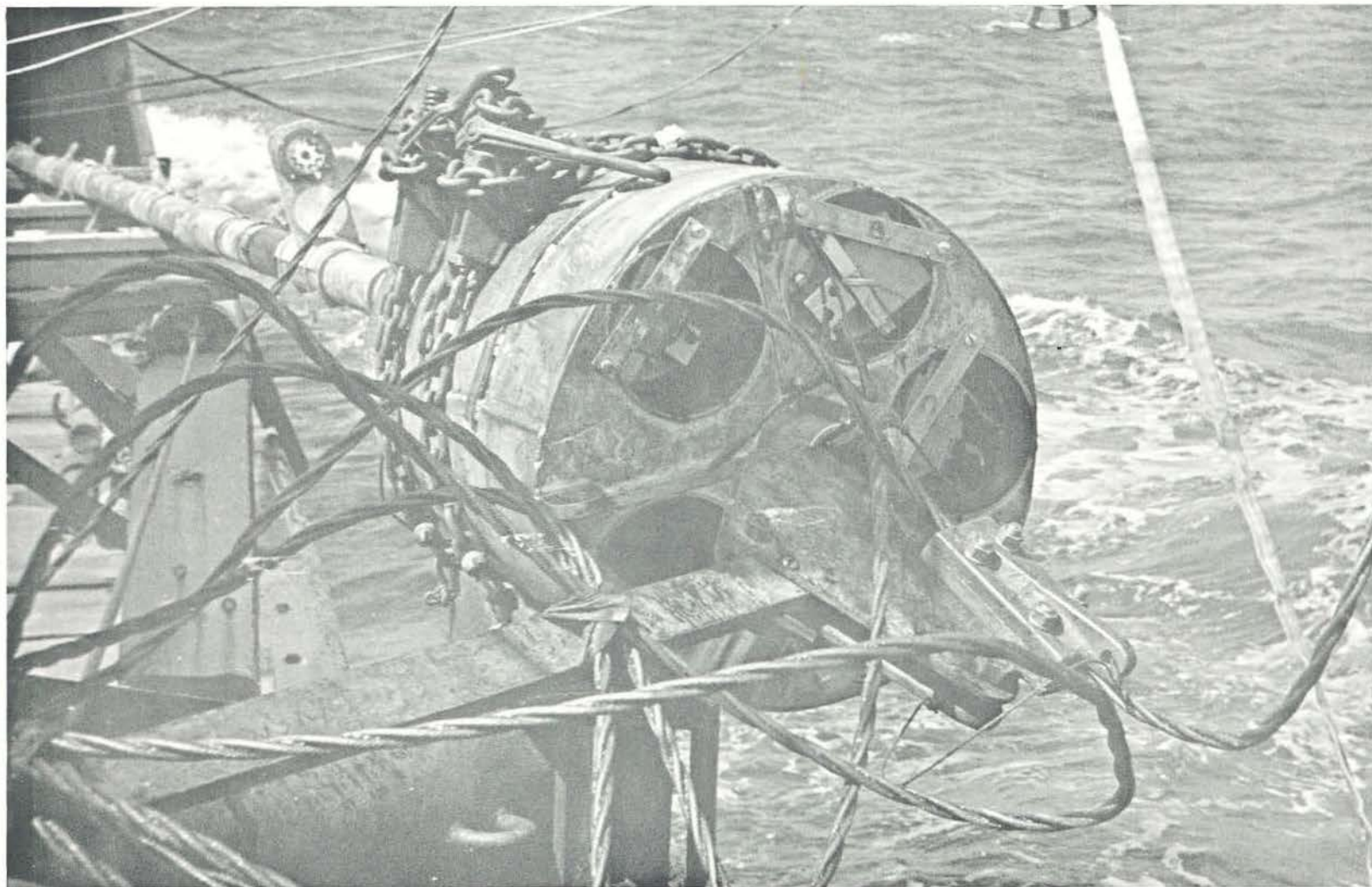


Figure 2. Piston corer and instrumentation prior to a lowering. The two cameras are mounted within the corehead at the upper left and at the right; the light source is mounted between the cameras. A heat flow recorder is mounted in one of the two lower cavities. The compass and inclinometer are shown attached to the core barrel below the corehead. Photo by C. Hilliard.

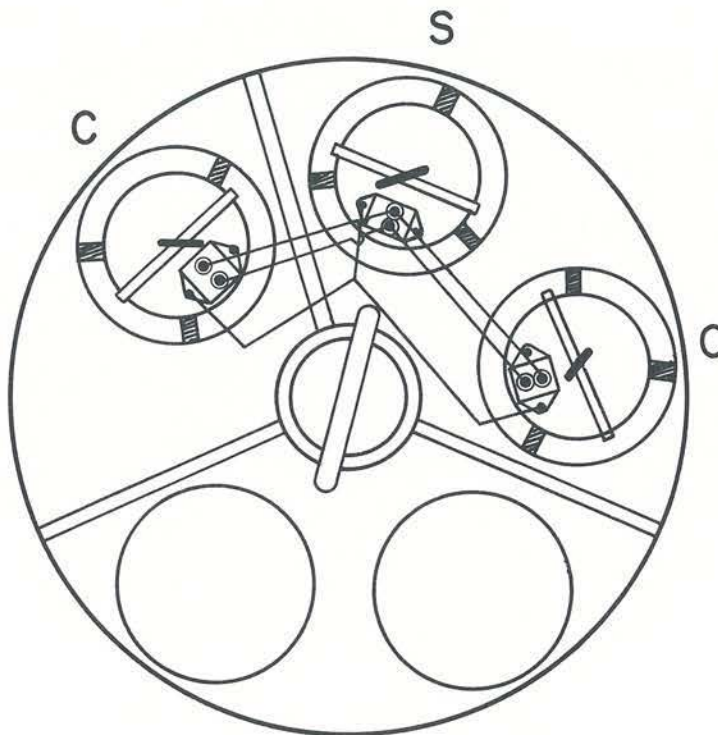


Figure 3. Exterior electrical connections between the cameras ("C") and the light source ("S"), as seen looking down on the top of the corehead.

Preliminary tests conducted in a clear pond gave exposure information which was later confirmed in deep water under actual operating conditions at sea. The aperture settings used are listed in Table II, including the settings for the data lenses.

Table II

Corehead camera aperture settings

	Hopkins adjustable aperture lenses		data lenses	
	Tri-X [*]	Plus-X ^{**}	Tri-X [*]	Plus-X ^{**}
camera focused at 1.8 m (6 ft)	f/22	f/16	f/4	f/2.5
camera focused at 4.9 m (16 ft)	f/6.3	f/5.0	f/4	f/2.5

* Kodak panchromatic Tri-X film rated at ASA 400

** Kodak panchromatic Plus-X film rated at ASA 125

Coring Apparatus

A completely new design for a corehead was necessary to fulfill two basic requirements: (1) additional overall weight greater than that which had been previously used, and (2) five cylindrical receptacles to accommodate the two cameras, the strobe-light source and two other instruments. The general design and specifications of the new corer are shown in figure 4. Emphasis was placed on maintaining as small an overall size for the corehead as possible to facilitate handling aboard ship, but still allowing the use of existing E. G. & G. cameras, strobe lights, and other instruments. Since a compass would be mounted 1.5 m (5 ft) beneath the corehead, non-magnetic no. 304 stainless steel was used in constructing the exterior and interior shell of the corehead. This was subsequently filled with lead.

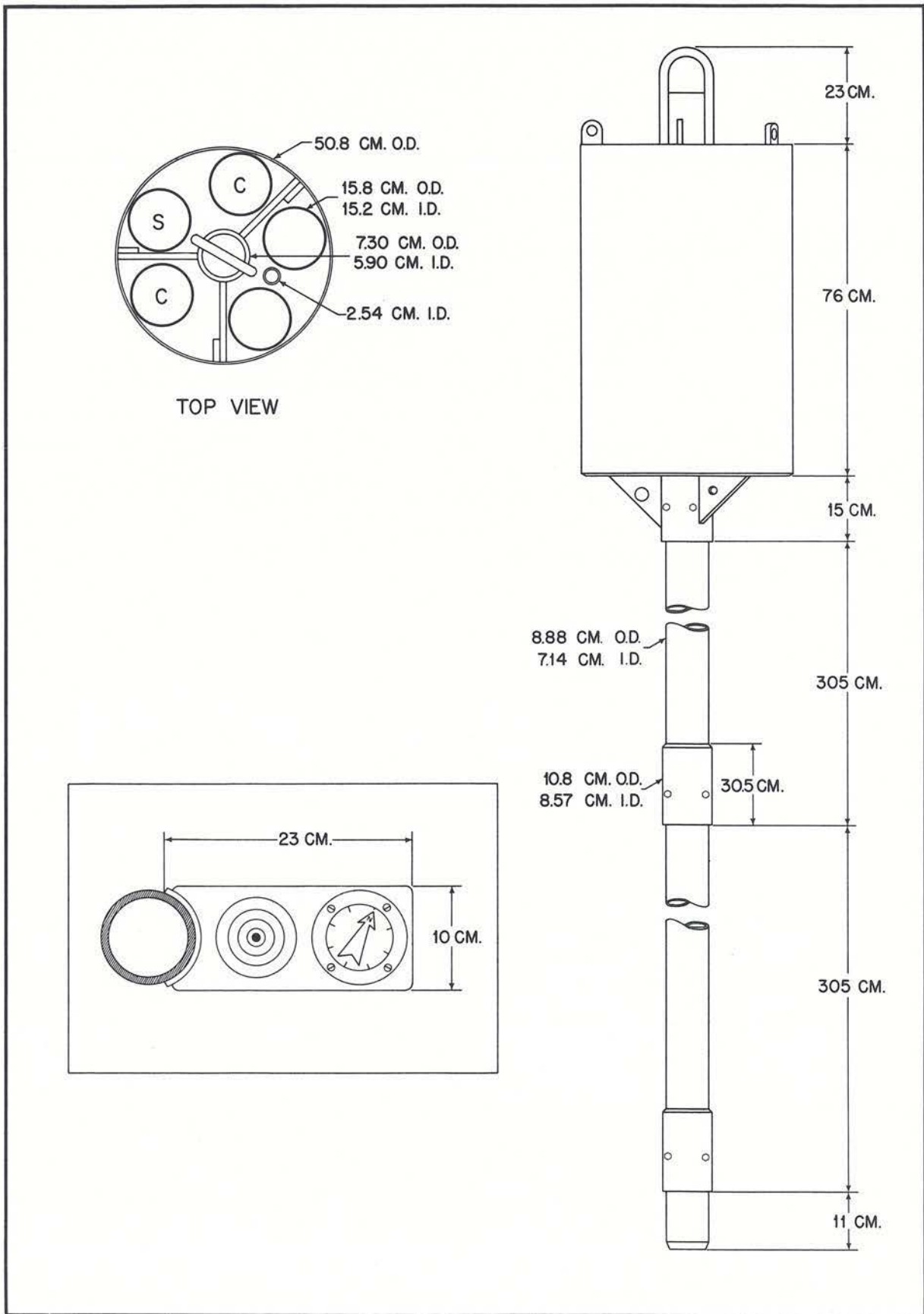


Figure 4. Specifications of the corehead and core barrels. In the top view, the positions of the cameras ("C") and light source ("S") in the corehead are shown. The inset at lower left gives the dimensions of bracket arm holding the inclinometer (left) and the compass (right).

To determine the orientation and vertical deviation of the corer, a compass and inclinometer were mounted on a bracket arm (see figures 2 and 4) that was attached to the upper core barrel 1.5 m beneath the corehead by large U-shaped bolts. The compass was a Model 2967 Mate Marine Compass (Taylor Instrument Co.) with a compass card graduated in 5° divisions and a small north arrow. This compass card, however, was found to be unsatisfactory if the water was murky or if the camera focused at 1.8 m did not operate. Consequently, a compass card with a large north arrow was used that was clearly visible in the photographs from both cameras (see inset, figure 4).

To construct an inclinometer for recording the deviation from vertical of the corer, a cast acrylic rod 8.26 cm (3.25 in) in diameter was cut 1.59 cm (0.625 in) thick. A 6.03 cm (2.375 in) diameter depression was machined into its center and the base of the depression was rounded to a radius of approximately 58 cm (23 in). A cover 9.5 mm (0.375 in) thick was cut from the acrylic rod and scribed with three blackened concentric rings calibrated in 5° steps (see inset, figure 4). The inclinometer was filled with kerosene and an 8 mm (0.3 in) diameter stainless steel ball was used as an indicator within the inclinometer. The back of the inclinometer was painted white for maximum contrast.

The aluminum bracket holding both the compass and the inclinometer was aligned with the metal strengthening rib between the strobe-light and the camera focused at 1.8 m; figure 5 illustrates this positioning of the bracket arm.

When fully rigged and equipped with instruments in all five corehead cavities, the corehead weighed approximately 910 kg, in air; each core barrel section weighed approximately 55 kg. The completely equipped corer with heat flow equipment mounted along the barrels is shown in figure 2.

Corer Design

The effectiveness of a corer, according to Hvorslev (1949), could be described by considering three ratios that involve the inside and outside diameters of the core barrels and the core cutter: the inside

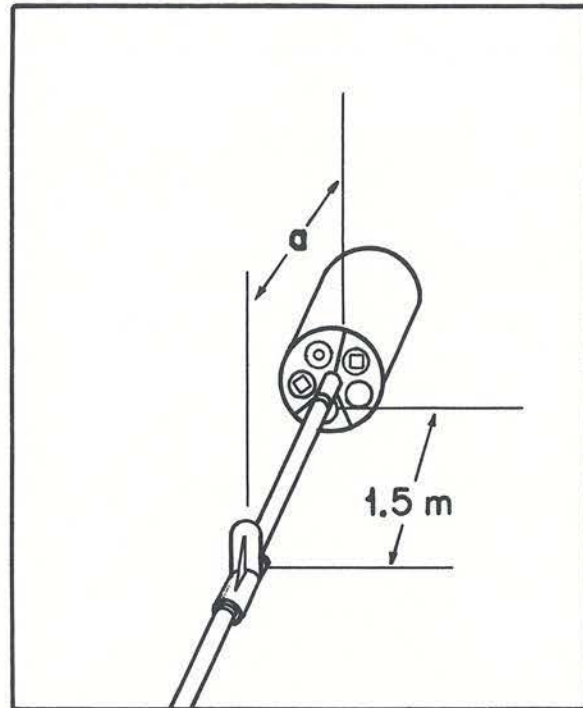


Figure 5. Diagram illustrating the positioning of the bracket arm holding the compass and inclinometer beneath the corehead. The bracket arm was attached 1.5 m below the corehead, as measured from the base of the adaptor coupling on the corehead to the upper surface of the bracket arm mount, and in line with the metal strengthening rib between the strobe light (upper left) and the camera focused at 1.8 m (upper right). This alignment is shown by "a"; the azimuth of this alignment was used to determine the piston corer's orientation.

clearance ratio, C_i , which describes the friction within the core barrel; the outside clearance ratio, C_o , which described the friction along the outside of the core barrel, and the ratio of the volume of displaced sediment to the volume of the sample, C_a . These ratios are defined in Table III.

For coring in cohesive sediments, Hvorslev (1949) recommended that the ratios (expressed as percentages) for C_i , C_o , and C_a be 0.75-1.5%, < 3%, and < 10%, respectively. Table III compares these recommended

Table III

Hvorslev's Ratios of the Piston Corer

	This Corer		Hvorslev's Recommended Values
	considering couplings	not considering couplings	
C_i^*	0	0	0.75-1.5%
C_o^{**}	21.4%	0	< 3%
C_a^{***}	176%	87%	< 10%

$$*C_i = \frac{D_s - D_e}{D_e}$$

D_s = minimum inside diameter of core barrel (including core liners)

D_e = minimum inside diameter of the nose cone

D_w = outside diameter of the nose cone

D_t = outside diameter of the core barrel

$$**C_o = \frac{D_w - D_t}{D_t}$$

$$***C_a = \frac{\frac{D_w^2}{2} - \frac{D_e^2}{2}}{D_e^2}$$

values with the values calculated for the corer used with the corehead cameras. Couplings are considered in Table III because the core nose protrudes 11 cm (4.25 in) below the last coupling (see figure 4). The calculated values for Hvorslev's ratios indicate that: (1) with respect to C_i the corer is well designed, (2) with respect to C_o it is also well designed unless the lower coupling is considered, but (3) with respect to C_a , the corer is very poorly designed.

Diagrams published by Ross and Riedel (1967) indicate that with values for C_o and C_i approaching values suggested by Hvorslev the amount of core shortening will be minimal. Hvorslev's recommended values, however, were based upon tests conducted in sediments having a uniform water content with depth; this frequently is not the situation in deep-sea sediments. Piston corers are designed to minimize C_i , so that this value might not be too applicable in comparing various piston corers. Values for C_a do not apparently affect core shortening in open-barreled gravity corers, according to Ross and Riedel (1967, figure 3c), and where a piston is used, larger values of C_a may be satisfactory (Hvorslev, 1949). These parameters are only partly useful in describing a corer's efficiency for bottom sampling because of the many other factors involved, such as, for example, the weight of the corer, the positioning and stability of the piston, the character of the sediment, and the velocity of the corer after free-fall (Emery and Dietz, 1941).

Shipboard Operation

With the exception of the first two stations, at least four or five heat-flow thermistors were mounted along the core barrels at each station on CHAIN cruise 75. The compass-inclinometer bracket arm was always mounted in the same position (figure 5). For sample orientations, each core liner was scribed with a straight line that was also aligned with the bracket arm.

The pilot corer was rigged to give the piston corer about 6.7 m (22 ft) of free-fall. Accordingly, 6.7 m of winch wire was coiled on the tripping arm plus an additional amount to account for the upward response of the cable to the impulse produced by the release of the piston corer, or cable rebound (see Section IV). Total lengths of 5.2, 6.7, 8.2, 9.2 and 12.2 m of winch wire were used, corresponding to -1.5, 0, 1.5, 2.5, and 5.5 m of added winch wire to allow for cable rebound. These attempts at immobilizing the piston at the sediment surface are further discussed in Section IV.

Immediately before the corer was lowered, a timer was set on the cameras for the proper time delay, as determined by the water depth. The connections between the cameras and strobe-light source were then completed, and the corer was ready.

The corer was lowered at about 100 m/min until it was about 200 m or less above the bottom. The lowering was then stopped with the corer held at this depth until the cameras had started running and an additional five minute time delay had elapsed to allow the light-fogged film leader to run through the cameras. The corer was then slowly lowered until the tensiometer or a pinger mounted within the corehead indicated that it had tripped. The winch was immediately stopped. The corer was left in the bottom for about 5 minutes; winch wire was slowly played out whenever tension increased on the wire.

Pull-out was accomplished by bringing in winch wire as slowly as possible until the tensiometer indicated that the piston corer was free of the bottom. The winch speed was then increased to about 100 m/min and the corer brought back to the surface.

III. OPERATION OF THE PISTON CORER

Introduction

The photographs taken by the corehead cameras provide a convenient method for studying the operation of a piston corer. In this section, we shall discuss the photographic evidence relating to these operations and compare them to previously published theoretical studies and shipboard procedures. The results of the coring operation, such as the length of core retrieved, disturbances in the core, etc., will be discussed in Section IV. As noted earlier, over 19,000 photographs were taken by this corehead camera arrangement on CHAIN cruise 75, all of which were studied to provide data on the operation of the piston corer; corehead camera photographs from ATLANTIS II cruise 42 were also studied.

Descent

Most of the descent photographs were taken while the corer was being held above the bottom and while it was slowly being lowered at speeds of about 20 m/min or, in a few cases, at about 40 m/min. On only one station (station 2) were photographs taken while the corer was descending at speeds of about 80 m/min.

The corer orientation and vertical showed no significant differences or variations between the time periods when the corer was being held above the bottom or descending at various rates. Descent, as used here, will therefore describe the time prior to the corer's tripping regardless of the rate of lowering.

In general, the corer orientation was very stable during descent. The average variation in orientation was only about 5-10° per 5 second interval in no preferred direction. On one station where the corer pretripped the maximum variation was 70° per 5 second interval, and on one station where slightly bent barrels were used this variation was as much as 120° per 5 second interval. The average orientation during descent for 33 stations is shown in figure 6 with a wind rose for these stations. There appears to be a correlation between the dominant wind direction and the orientation of the corer on some of the stations, with the tripping arm acting as a vane to produce this orientation while the ship drifts (a method sometimes used to estimate core orientations; see, for example, Ewing, et al., 1967).

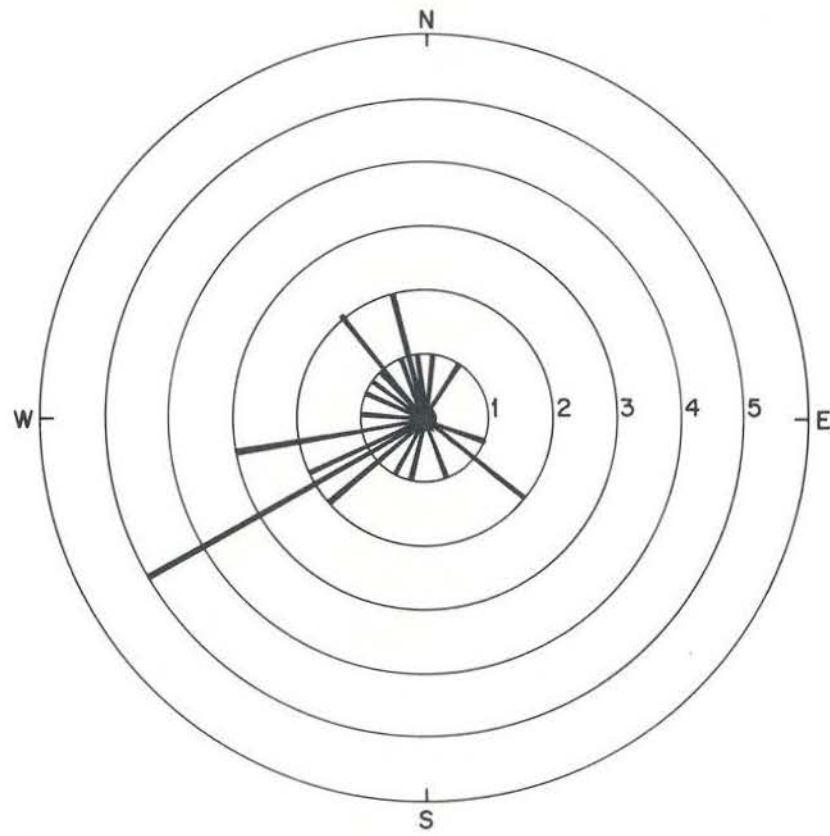
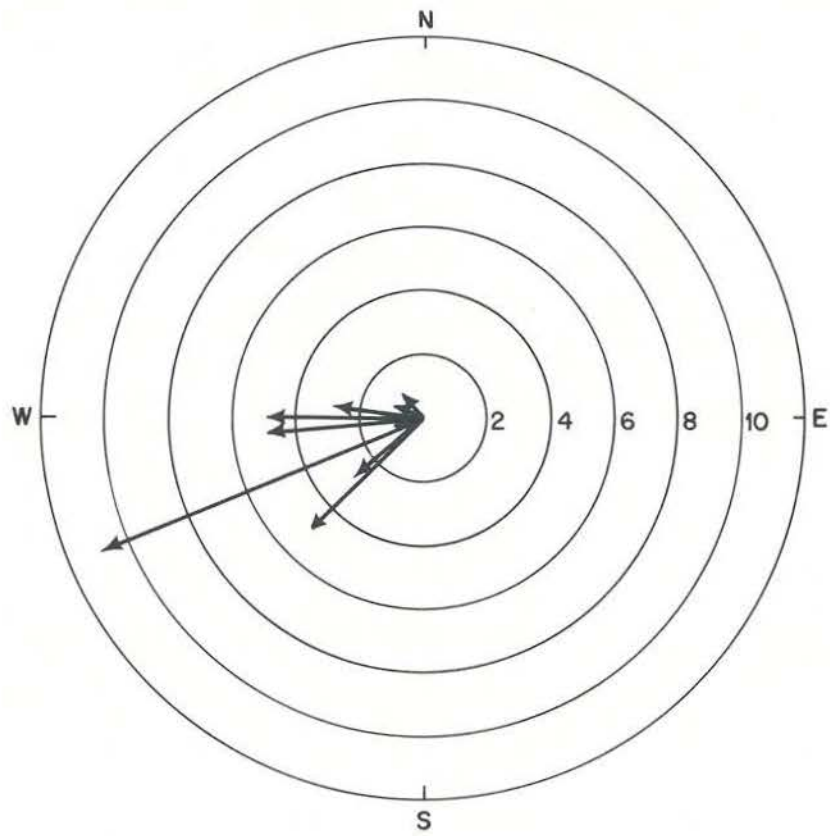


Figure 6. (Upper) Wind direction during 33 coring stations on CHAIN cruise 75. (Lower) The average azimuth of the tripping arm during descent on these 33 stations. Concentric circles give the number of occurrences; thus on 11 stations the wind was from the ENE and on 5 stations the corer orientation was 240°

During twelve coring stations on which the ship was allowed to drift, however, the deviation between the direction of ship's drift (assuming a parallelism between wind direction and ship's drift) and the azimuth of the tripping arm varied considerably, seven of the stations having a deviation of 10° - 40° (figure 7). The lack of pronounced orientation of the tripping arm with respect to drift may have been due to the relatively heavy piston corer used. Average wind velocity on all stations was about 10-15 knots.

The average deviation from vertical of the piston corer during descent also varied very little on a particular station and consistently remained about 6° in the same direction. On each station the average variation was less than 2° during descent, with a maximum variation of 10° on one station. There was no relationship between this average deviation and either the number of instruments mounted within the corehead or the number of core barrels attached. During ATLANTIS II cruise 42, wind velocities were generally lower than those during CHAIN cruise 75, and the deviation from vertical during the ATLANTIS II cruise was considerably less, averaging only about 1 - 3° . Since a different corehead was used on the ATLANTIS II cruise, and since the deviation of the corer used during the CHAIN cruise was 0° when suspended in air with one core barrel, we believe that this consistent deviation from vertical of the CHAIN corer during descent was probably the result of relative horizontal motion of the corer through the water. If the deviation from vertical were a function of the number of core barrels attached, then it should decrease when the barrels contained a sample; instead, it usually increased slightly during ascent.

Tripping and Free-Fall

The identification of photographs that might have been taken at the moment the corer was tripped or during its free-fall is extremely difficult. Slight changes in the corer's orientation and deviation from vertical probably would occur, as usually did happen during penetration. But, because such changes in the corer's attitude were not noticed, no photographs evidently recorded the free-fall of the corer. Usually the first bottom photograph showed the corer penetrating or to have completely penetrated into the bottom, suggesting that the time for free-fall and partial or complete penetration was less than 5 seconds, the time lapse between photographs. A pinger mounted within the corehead on 14 stations indicated that free-fall took about $1 \frac{1}{2}$ seconds. Such a short time for free-fall agrees well with theoretical estimates.

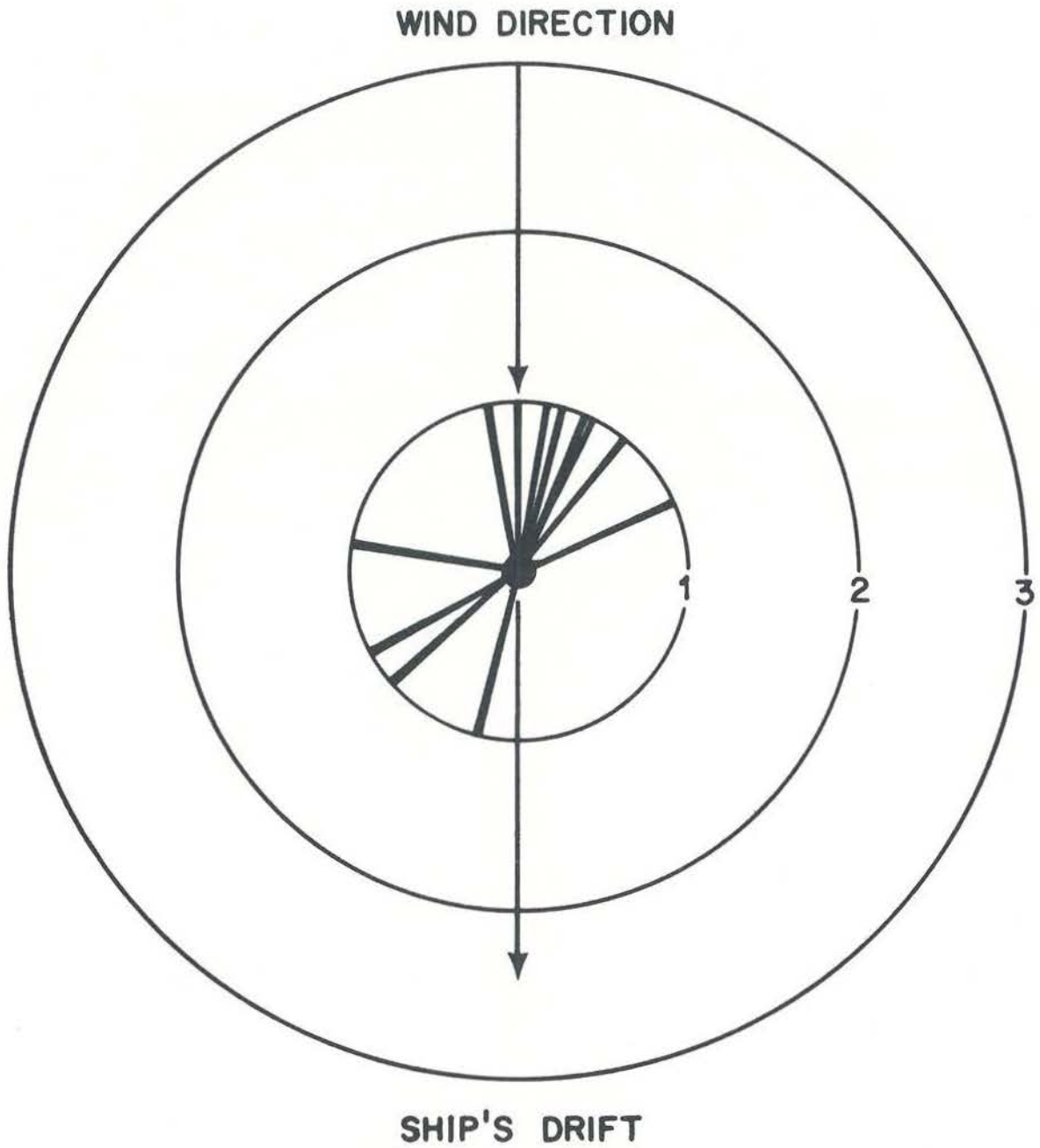


Figure 7. Deviation of the azimuth of the tripping arm from the wind direction and presumed direction of ship's drift during 12 coring stations where the ship was allowed to drift throughout the station. Concentric circles are the number of occurrences. Thus, the orientation of the tripping arm was parallel to the presumed ship's drift during only one station.

Theoretically, the time for free-fall of the piston corer in water with its nose cone 6.7 m (22 ft) above the bottom would be slightly over one second. For example, for a drop of 6.7 m Hvorslev and Stetson (1946) calculated a time of about 1.3 or 1.4 seconds for a 454 kg corer (about half the weight of the corer used in this study) and Burns (1966) experimentally measured a time of 1.7 seconds for considerably lighter corers weighing 25 to 54 kg. Applying the equations of Kullenberg (1955) to the heavier corer described here, with a free drop of 6.7 m and a slight correction for buoyancy, the time for free-fall would be about 1.25 seconds (figure 8).

The maximum velocity of the corer during free-fall and the weight of the corer are important factors in determining the amount of penetration; generally, higher velocities and heavier corers result in increased penetration (Emery and Dietz, 1941; Hvorslev and Stetson, 1946). The maximum velocity during this brief time of free-fall can be calculated from equations given by Kullenberg (1955), and would be about 8 m/sec for the corer carrying the corehead cameras. These equations indicate that a fall of greater than about 8-10 m would not significantly increase the final velocity; in fact a greater height would probably only encourage rotation and perhaps tumbling during free-fall, as also noted by Kullenberg (1955) and Burns (1966). Significant variations in velocity might be introduced by vertical oscillations of both the cable and corer during descent. Lister (1964) has found vertical oscillations of as much as 2 m for a 454 kg corer at the end of about 450 m of 1.27 cm (1/2 in) diameter cable. Kullenberg (1955) calculated vertical oscillations of over 2 m for a heavier corer (1500 kg) suspended from about 590 m of cable. Vertical oscillations of similar, if not greater, amplitudes were also noted during the CHAIN 75 lowerings from records produced by a pinger mounted within the corehead. Such oscillations would not be seen in mid-water photographs taken by the corehead cameras, although periodic sediment discharges from the corer during ascent and the slight variations in vertical deviation and orientation during both descent and ascent may have been partly caused by these vertical oscillations.

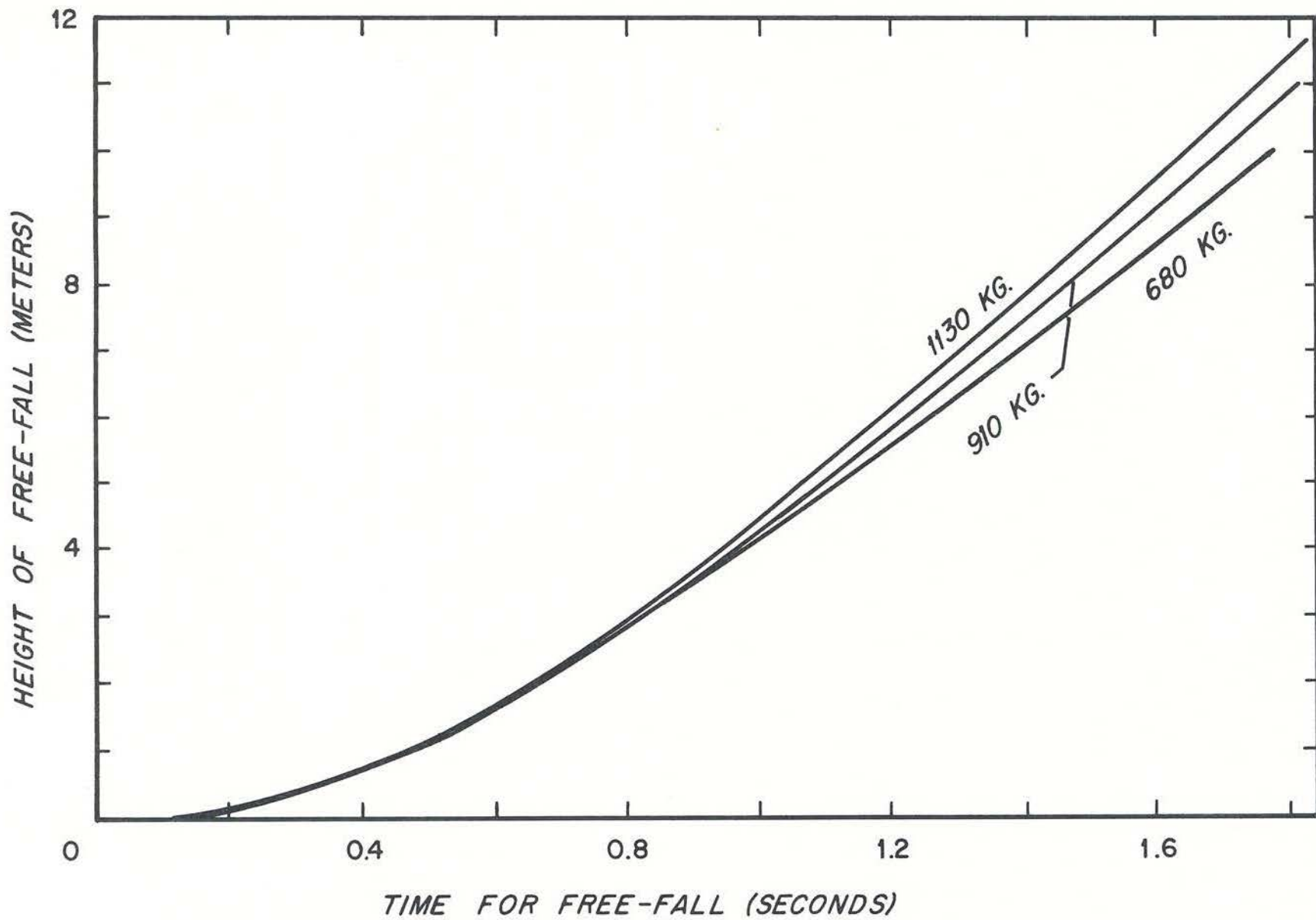


Figure 8. Time for completion of free-fall with respect to the height of the corer above the bottom, or the distance of free-fall, as calculated for three corers of different weights from the equations given by Kullenberg (1955).

Penetration

Photographs on eleven stations recorded the initial, high velocity penetration of the piston corer into the bottom. Clear photographs showing this penetration were taken on six stations, three of which are shown in figures 9, 10, and 11. Photographs taken on the other five stations indicated penetration was in progress from the murky, turbulent water obscuring the bottom followed by blank pictures taken after the camera lenses were buried in mud. Slowly continuing penetration as the corer settled into the bottom was photographed on five additional stations. On the remaining stations where bottom photographs were obtained, the first bottom photograph apparently was taken after maximum penetration had been completed.

Rotation of the corer during free-fall and penetration was indicated on 13 out of 14 stations where a comparison could be made between the average orientation of the corer during descent and the orientation of the corer in the bottom. On only four of these 13 stations was this rotation less than the average rotation during descent. On the remaining nine stations a rotation of 20° to 60° occurred during free-fall and penetration, with an average rotation of 30°, in no preferred direction. Photographs from ATLANTIS II cruise 42 also indicated a similar amount of rotation. This motion may twist the liners within the core barrels out of alignment, if the piston does not rotate with the corer. Black spiral marks left by the rubber gasket of the piston on the liners during one coring station on ATLANTIS II cruise 42 indicated that this does occur. Determinations of the magnetic declination on some CHAIN cruise 61 piston cores have indicated a rotation of up to 55° between liners.

An average increase of 6° in the deviation of the core barrel from vertical occurred during penetration for all of the 14 stations mentioned above. In every case, the vertical deviation in the bottom was larger than that recorded during the corer's descent. On five additional stations a significant increase was noted just prior to the inclinometer being buried. These apparent increases may have been partly produced by the impact of the corer with the bottom; for example, on station 45 the apparent deviation increased from 6° to 18° with impact but then remained at 12° after penetration was completed. Photographs from ATLANTIS II cruise 42 indicated a slightly lower increase.

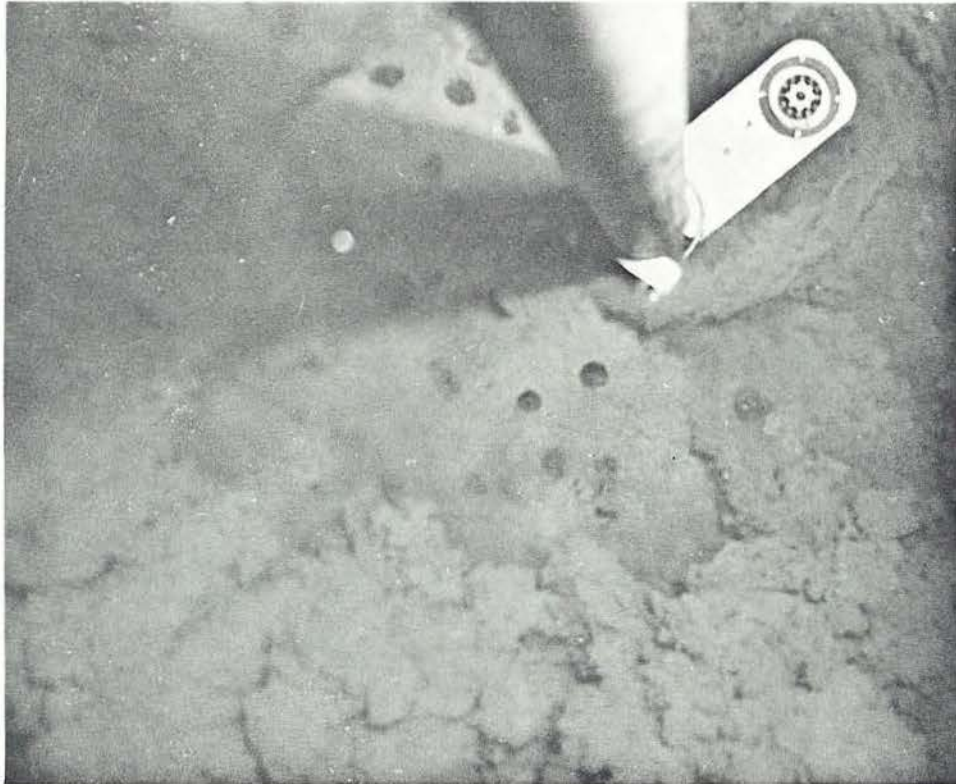


Figure 9. Penetration of the piston corer into the bottom on station 2. The larger, dark particles on the sea-floor around the core barrel are probably manganese nodules. Penetration continued to about 1 m from the corehead (see figure 17) burying the bracket arm. Photograph taken by the camera focused at 4.9 m (16 ft).



Figure 10. Penetration of the piston corer into the bottom on station 17. Note sediment cloud produced by the corer upon impact with the bottom. Penetration continued to about 60 cm from the corehead, burying the bracket arm and the other instruments mounted opposite the bracket arm. Photograph taken by the camera focused at 4.9 m (16 ft).



Figure 11. Penetration of the piston corer into the bottom on station 31. Penetration continued to about 90 cm from the corehead, burying the bracket arm. Photograph taken by the camera focused at 1.8 m (6 ft). The vertical deviation of the corer during penetration is 10° , as recorded by the inclinometer.

Penetration and free-fall was usually accomplished within one or two pictures, that is, in about 10 seconds or less. This time varied considerably from less than 5 seconds on 11 stations to 5 minutes on one station (station 11), where the corer slowly but continually penetrated throughout the station. As noted in the previous section, free-fall was completed in slightly over 1 second, thus penetration was completed in less than 4 seconds on eleven stations, and less than 9 seconds on eight stations.

It is extremely difficult to theoretically determine the time for penetration because of the many variables involved, such as, the weight of the corer, its velocity upon penetration, the varying depth of penetration, the design of the corer, and the frictional resistance of the sediment. The frictional resistance alone is highly variable depending upon the sequence and character of the bottom sediment with grain size variations, water content, etc. (Emery and Dietz, 1941) and probably increases with increasing penetration (Hvorslev and Stetson, 1946). Because of these variables, no accurate value of frictional resistance can be calculated. Hvorslev and Stetson (1946) believe that the time for penetration can be approximated, however, by:

$$T_p = \frac{2D}{v} \quad \text{where } D \text{ is the total length of coring barrels attached and } v \text{ is}$$

the velocity upon impact. Assuming an impact velocity of 8 m/sec, about 3 seconds would be required for complete penetration by an 1130 kg corer, the weight in air of the corer which carried the corehead cameras (figure 12). If about 1.5 seconds is required for free-fall and 3 seconds is required for penetration, then free-fall and penetration would take place within the time span between pictures or about 5 seconds. This approximation agrees with the photographic evidence on at least eleven stations. The longer time required for penetration on the remaining stations probably can be accounted for by the range of variables mentioned above. It should be noted that the corer always had at least five exterior heat-flow thermistors attached, thereby significantly increasing the cross-sectional area of the penetrating corer.

The amount of penetration could be measured from bottom photographs on twenty stations (see Table IV). On nine other stations the amount of penetration could only be estimated due to the corehead entering the sediment and burying the camera lenses. Penetration could not be measured on the remainder of the stations because of poor bottom photographs,

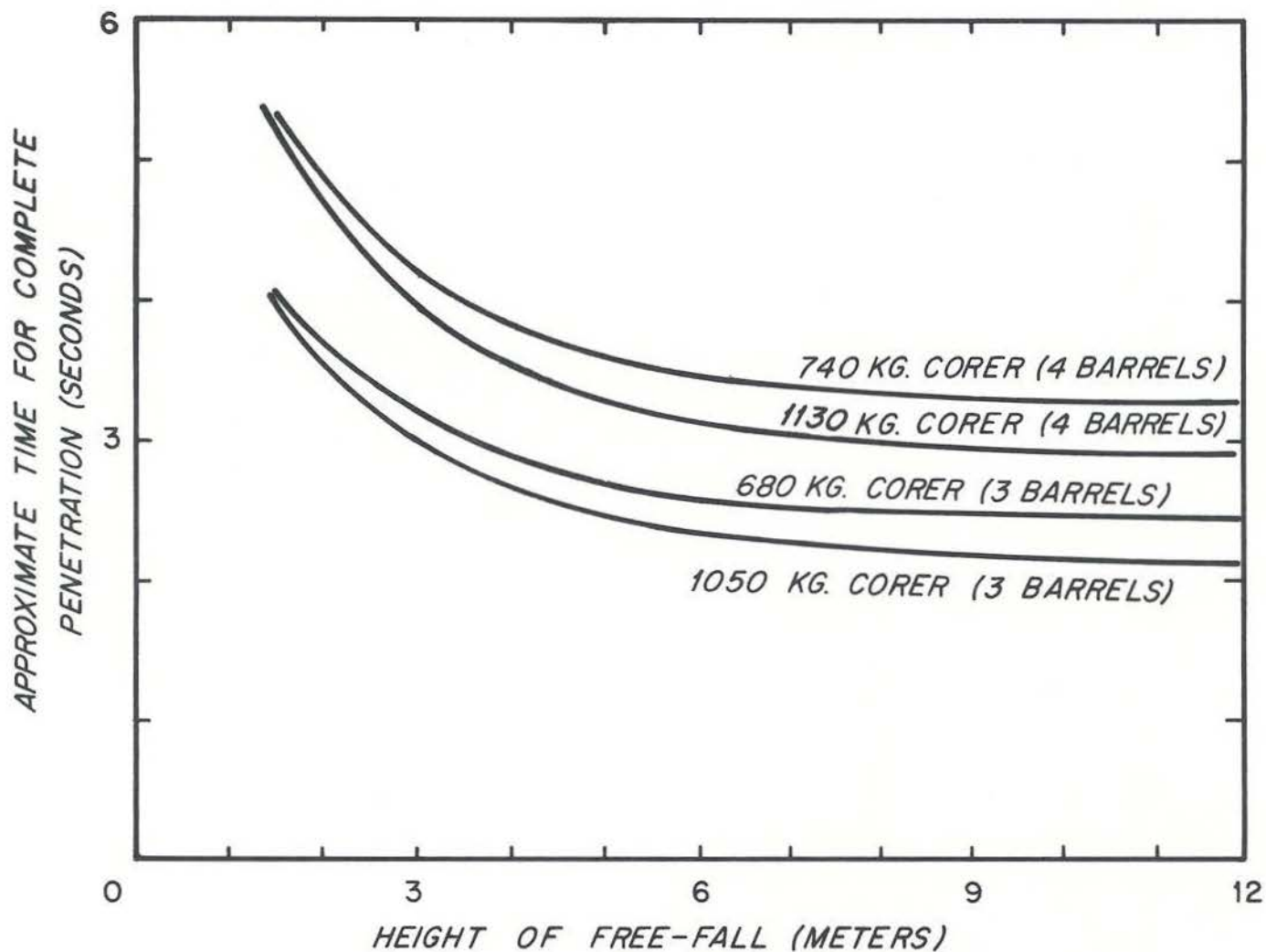


Figure 12. Approximate time for complete penetration of a corer into the bottom following free-fall as a function of the height of free-fall, according to the relationship given by Hvorslev and Stetson (1946). The four curves represent two different corers, first with 3 core barrels attached, then with 4 core barrels attached. Assumed velocity at impact is 8 m/sec.

the corer bending, a hard bottom, or camera failures (see Table I). Generally, a greater penetration was achieved in the predominantly red muds of the abyssal plain. The angle at which the corer penetrated appeared to have no relationship to the depth of penetration, at least within the 0-18° angle that the inclinometer measured. A further discussion of penetration, including the method used to determine the amount of penetration, will be given in Section IV.

Upon impact with the bottom, a symmetrical, dense, turbulent doughnut-shaped cloud 30 to 100 cm high was produced around the core barrel (figures 10 and 11). If bottom currents were present, the cloud was asymmetric in the direction of the current (McCoy, 1969); in only one case was this asymmetry apparently produced by the angle at which the corer entered the bottom. Where bottom currents were present, the cloud dispersed within 15 seconds, but in the absence of strong bottom currents the water often would remain murky throughout the time on bottom (approximately 5 minutes). The cloud advanced initially at a velocity of about 4.5 cm/sec on station 32, where no bottom currents were apparently present. During station 38, a 1-3 cm/sec bottom current was flowing and the advance of the cloud could be followed in the direction of the bottom current for 25 seconds (5 photographs) giving velocities of 6.6, 6.1, 5.7, and 3.6 cm/sec, although velocities within the cloud were undoubtedly much higher because of the internal turbulent motion. Ewing, Hayes and Thorndike (1967) estimate velocities on the order of 100-200 cm/sec about 50 cm from the corer, adequate for removing manganese nodules near the corer. Such high velocities do not seem to have occurred with this corer; what appear to be manganese nodules were photographed on station 2 (figures 9 and 13) and they do not appear to have been moved.

The sediment cloud was probably produced by both the lateral dispersion of water trapped within the nose cone of the corer and by the impact of the core barrel with the bottom. About 400 cubic cm of water would be trapped between the core cutter and the piston, and would probably be expelled laterally by sediment entering the core barrel after penetration if the piston had not yet begun to move.

Corresponding disturbances of the sea floor around the barrels were noticed on every station where clear bottom photographs were taken. Most frequently, mounds of sediment 7 to 10 cm high extended out over 30 cm from the core barrel, or from the bracket arm if it also entered



Figure 13. Small manganese nodules near the core barrel on station 2. Penetration has been completed here; figure 9 shows the corer in the process of penetration. These nodules have not been disturbed by the corer during penetration, as can be seen by comparing this photograph with figure 9. Note the cable lying on the bottom. Photograph taken by the camera focused at 4.9 m (16 ft).

the bottom, obliterating most bottom features within the area of the bottom photograph. Figures 14 and 15 are examples of mounds on stations 37 and 46. The cohesive texture of some of the sediment forming the mounds, such as in figures 14 and 15, suggest that this material has been forcefully pushed aside, perhaps by the piston penetrating some distance into the bottom before being immobilized. A few have been cut by small channels (figure 16) suggesting that the channels have been eroded by the lateral dispersion of trapped water within the nose cone, after the mounds were formed. The extremities of the mounds may have been produced by a combination of sediment thrown out during impact and by sedimentation from the turbulent sediment cloud.

Depressions around the core barrel were noticed on a few stations. The largest had a depth of about 15 cm and a diameter of about 40 cm. Figure 17 shows a depression on station 7; the apparently undistorted worm burrows exposed on the sides of the depression suggest that the depression was partly produced by erosion during the lateral dispersion of water. Downward deflection of sediment by the friction between the penetrating barrels and the sediment may also partly account for these depressions. On a few stations, the bottom was disturbed as much as 60 or 100 cm away from the corer, but whether this disturbance is a thin covering of sediment or a shallow depression cannot be determined.

The pilot corer was seen after penetration very close to the piston corer on a few stations during the CHAIN 75 cruise (figure 18), and frequently on the ATLANTIS II-42 cruise. Where it was visible, its angle of penetration and depth of penetration varied considerably, from a vertical position with maximum penetration to a considerable vertical deviation with only a slight amount of penetration. Since the untripped coring rig was usually lowered at about a speed of 30 cm/sec, the pilot corer would also penetrate at this velocity. However, the extreme vertical oscillations of the cable and the rebound of the cable (discussed in Section IV) could seriously alter this velocity, thereby accounting for the variable depths of penetration noted in the photographs. A higher diffuse sediment cloud noticed on three stations during CHAIN 75 and on the majority of the ATLANTIS II-42 stations evidently was produced by murky water discharging from the top of the pilot corer during penetration; bottom currents then slowly carried it through the camera's field of view (McCoy, 1969). The most disastrous appearance of the



Figure 14. Portion of sediment mound surrounding core barrel on station 37. Rectangular hole to the left has been formed by the bracket arm. Photograph taken by the camera focused at 1.8 m (6 ft).

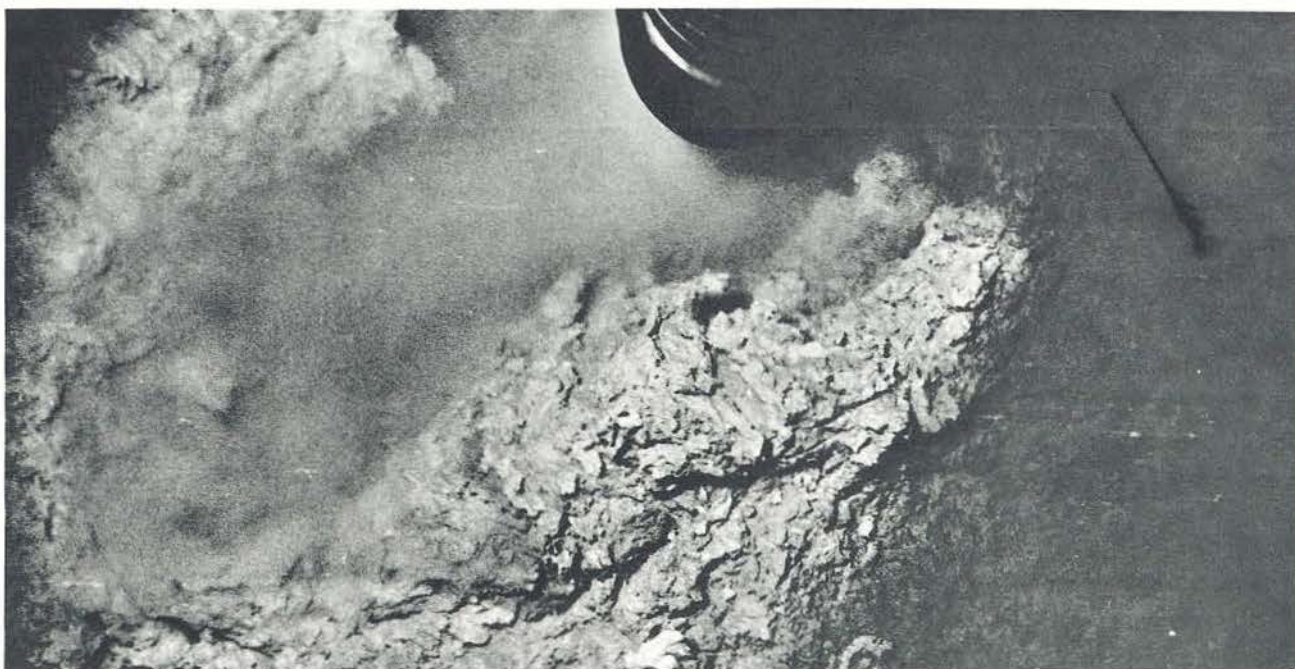


Figure 15. Portion of sediment mound surrounding core barrel and depression where bracket arm has plunged into the sediment (station 46). Photograph taken by the camera focused at 1.8 m (6 ft).



Figure 16. Sediment mound near the core barrel that has been cut by a small channel (station 17). Photograph taken by the camera focused at 1.8 m (6 ft).



Figure 17. Depression surrounding the core barrel on station 7. Note the worm burrows exposed on the slopes of the depression. The edge of the depression is difficult to distinguish in the photograph, but extends out to about the end of the bracket arm shadow; the long worm burrow near the shadow disappears into the sediment very near the edge of the depression. Photograph taken by the camera focused at 4.9 m (16 ft).



Figure 18. Pilot corer and piston corer in the bottom during station 14.
Photograph taken by the camera focused at 4.9 m (16 ft).

pilot corer during penetration was photographed on station 16, where either because of vertical oscillations or rebound of the cable, the pilot corer did not penetrate, and instead swung over on a taut tripping wire, smashing into the piston corer while it was penetrating and breaking the compass.

Motion While In Bottom

No rotation of the piston corer occurred after penetration had been completed during the 15 stations on CHAIN cruise 75 where the compass was visible throughout the station. The magnetic orientation of the corer in the bottom for these 15 stations is listed in Table IV. Only two exceptions were noticed: On station 32 the corer continuously rotated as much as 20° in no preferred direction for 50 seconds, then ceased to rotate for the remainder of the time on bottom. On station 45 a slow rotation of 10° occurred about midway through the station. Such disturbances could have been produced by slight pull-outs or by magnetic disturbances due to the piston, although neither the cable nor the piston seemed to affect the compass in tests on board the ship.

Swaying of the piston corer while in the bottom was noticed during only five stations, where changes of $2-9^\circ$ in the vertical deviation were recorded. A change of over 15° occurred during one station (45A). Any swaying of the corer while in the bottom enlarged the hole around the core barrel; this can be seen in figure 15.

Slight pull-outs of the piston corer were noticed on only four stations. Slow settling of the corer while it rested in the bottom occurred on five stations.

Poor penetration with four barrels attached to the corer caused severe bending of core barrels on stations 10 and 13 (figure 19). In both of these instances, the actual bending took place as much as 25 seconds after penetration, as recorded by a pinger mounted within the corehead. Bending was completed in 18 seconds during station 10, apparently immediately after 5 m of wire was played out to decrease the tension on the wire, and in 36 seconds during station 13. This bending was caused by failure of the coring barrels to support the heavy weight of the corehead; figure 20 gives the relationship between the extent of core barrel penetration and the angular deviation from vertical to cause bending. On both stations 10 and 13, the deviation from vertical was about 10° at impact with the



Figure 19. Photograph taken following the bending of the piston corer on station 10. The piston corer penetrated about 3 m before bending. The pilot corer penetrated about 90 cm, then fell over. Photograph taken by the camera focused at 1.8 m (6 ft).

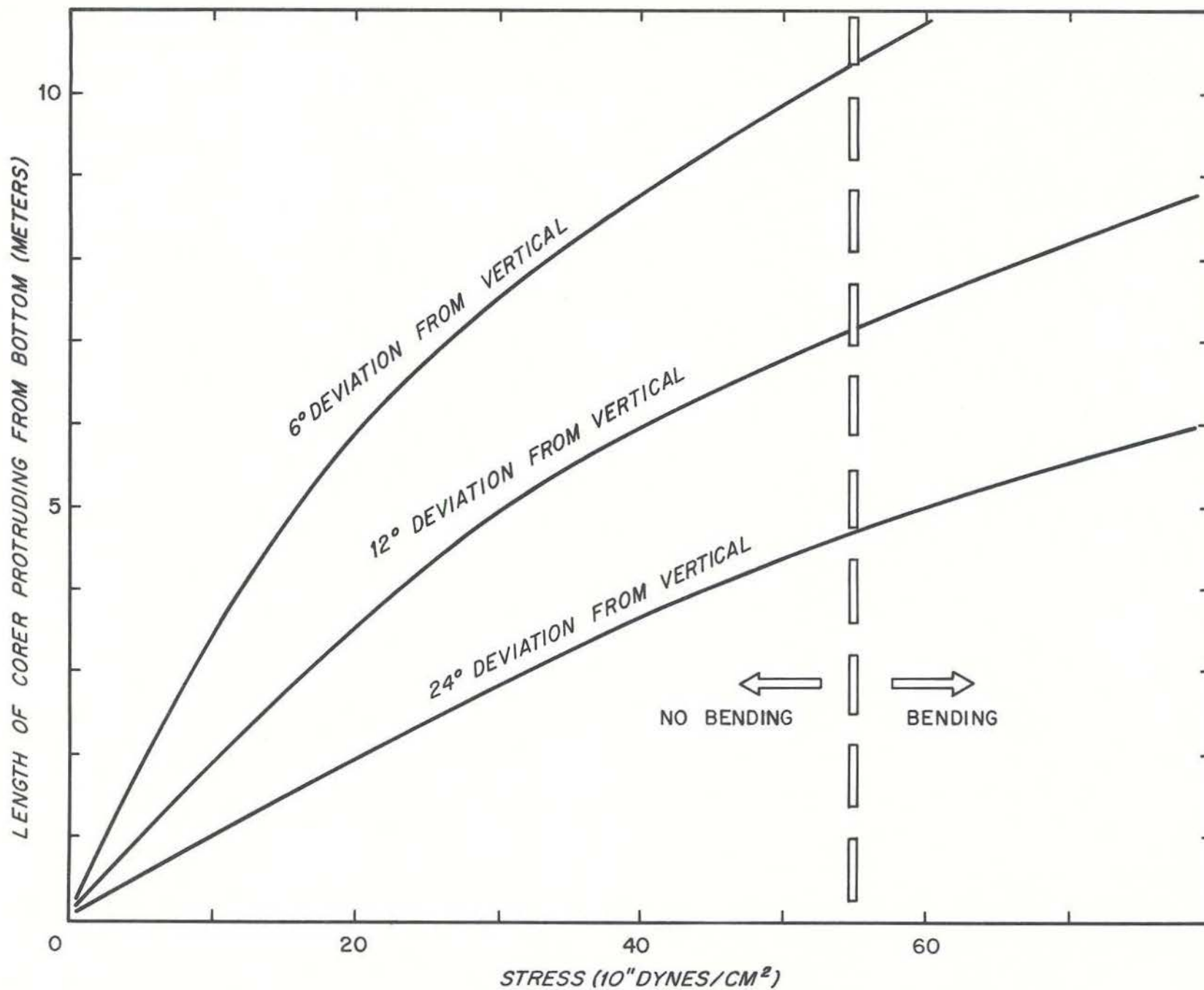


Figure 20. The calculated maximum stress at 6°, 12° and 24° deviations from vertical for various lengths of the corer protruding above the bottom. The coring barrels used during CHAIN cruise 75 had a yield stress of 55×10^{11} dynes/cm²; this is shown as the approximate boundary between bending and no bending of the corer.

bottom, and with a penetration of about 3 m on both stations, or with about 9 m of corer protruding from the bottom, the yield stress on the coring pipe was certainly exceeded according to figure 20.

The pilot corer was usually outside of the camera's field of view. It did appear abruptly during two stations. Poor penetration on station 18, and a broken coring tube on station 45, allowed the pilot corer to swing into view near the piston corer, evidently as wire tension between the ship and the corer increased. During station 18, the pilot corer continually circled and hit the piston corer; in figure 21 it has just come into view and appears to have partly penetrated.

Cable appeared in photographs on five stations (see figure 13). During stations 6 and 7, the tripping cable continually kept sweeping into view, often catching beneath the compass-inclinometer bracket arm and frequently twisted into a loop. On the three other stations, cable was photographed lying motionless on the bottom. During many of the coring stations on ATLANTIS II cruise 42, cable was seen both lying on the bottom and coiled around the piston corer (figure 22).

Pull-Out

The withdrawal of the piston corer from the bottom, or pull-out, was accomplished rapidly (Plate I), frequently in less than 10 seconds (18 stations) with a maximum time of 30 seconds (one station).

Rotation of the corer with pull-out occurred during 10 of the 11 stations where the withdrawal was photographed. The amount of rotation varied considerably: rotation on three stations was 115° - 165° , rotation on two stations was about 75° , and rotation on five stations was about 30° . This rotation was opposite to the lay of the winch cable on 6 of these stations.

Ascent

The corer was generally unstable during ascent, in contrast to the general stability of the corer during descent. In part this instability probably was initiated by the abrupt pull-out and the accompanying decrease in cable tension. Rotation and swinging of the corer immediately after pull-out was observed on 25 stations, but appeared to decrease in amplitude about 30 sec after pull-out on most stations.



Figure 21. Pilot corer resting on its side near the piston corer on station 18, after swinging around the piston corer. Photograph taken by the camera focused at 1.8 m (6 ft).

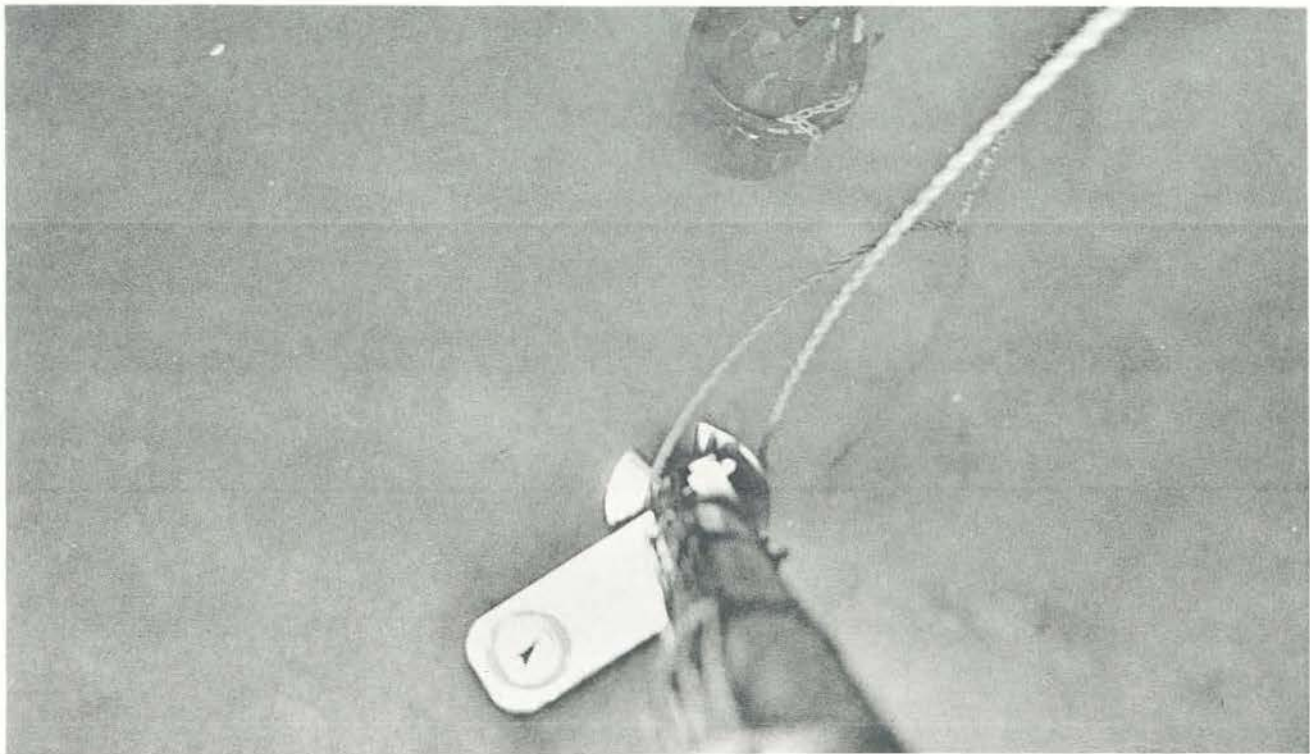


Figure 22. Winch cable wrapped around the piston corer during station 4, ATLANTIS II cruise 42. The narrow shield beneath the bracket arm was used in an attempt to inhibit penetration so that the compass and inclinometer would not be buried. Photograph taken by the camera focused at 4.9 m (16 ft).

Even with dampening of the more severe motions, the corer continued to rotate during ascent on 27 out of 30 stations, perhaps as a result of the relatively rapid hauling rate of about 100 m/min during ascent as well as a continuing response to pull-out. Usually the corer did tend to settle on two or three orientations but rarely did it consistently remain at this orientation. The average rate of rotation on a station varied from $40^\circ/5$ sec to $2^\circ/5$ sec, the maximum rate being as high as $175^\circ/5$ sec. In one case (station 10), an abrupt change in orientation corresponded to a change in winch speed.

On the majority of the 33 stations where the deviation from vertical was recorded during ascent, it increased by about 4° over the average during descent, frequently in the same direction. The maximum vertical deviation was 18° . The rate of variation averaged $5^\circ/5$ sec, with a maximum of $12^\circ/5$ sec, six stations recording no variation. This would suggest that little swinging of the corer occurs once it is dampened after pull-out, which is perhaps to be expected at the higher winch speeds.

Sediment discharges from the piston corer were often observed. These may have been produced by periodic sloughing of mud attached to the core barrels. In a few instances the discharge of sediment from the piston corer occurred after the pilot corer hit the piston corer.

With the faster winch speed during ascent and the tripped piston corer now hanging 5 to 9 m lower on the winch cable, the pilot corer frequently would swing in quite close to the piston corer (Plate I) and would occasionally hit the piston corer. The nearly continual rotation of the piston corer during ascent caused the pilot corer and the tripping cable to wrap around the piston corer on many stations.

Summary

Through the analysis of photographs taken by corehead cameras mounted on a piston corer, the operation of a piston corer designed according to the specifications given in Section II can be described as follows:

During descent, the corer is quite stable with little swinging and rotation, regardless of whether the corer is being lowered slowly or stopped in the water. Its orientation does not seem to reflect the ship's

drift. However, vertical oscillations of the heavy weight of the corer at the end of a long cable responding to ship's motion may result in vertical velocities as high as 200 cm/sec.

With tripping at a height of 6.7 m above the sea-floor the corer falls to the bottom in about 1 1/2 seconds, reaching a velocity of about 8 m/sec. This velocity will be slightly modified by the speed at which the corer is being lowered prior to tripping and significantly modified by vertical oscillations of the wire.

Full penetration of the piston corer into the bottom takes place in about 4 to 9 seconds, often allowing photographs to record this penetration; infrequently, further slower settling of the corer into the bottom may also take place. A rotation of 20-60° and an increase of about 6° in the vertical deviation occurs during free-fall and penetration. The amount of penetration does not seem to be controlled by this increase in deviation. Photographs taken during actual penetration show a large, symmetrical (providing bottom currents are absent), doughnut-shaped cloud raised by the impact. This cloud is evidently produced by the lateral dispersion of water trapped within the nose cone of the piston corer and within the interstices of the upper few centimeters of the bottom sediment. Disturbances of the surrounding sea floor in the form of mounds and depressions near the core barrel result from both this lateral dispersion of water and from the impact of the corer with the bottom. The depressions may also be due to a downward deflection of the bottom sediments. In the few cases where the pilot corer was seen, it had swung into view following poor penetration into the bottom.

While resting in the bottom, the piston corer is very stable although some wobbling does occur. Slight pull-outs were noticed on only a few stations. Bending of the corer on two stations evidently was the result of poor penetration and failure of the coring pipe to support the heavy core-head.

Pull-out was accomplished in about 10 seconds. Considerable rotation and a slight increase in vertical deviation accompanied pull-out.

During ascent, the piston corer is unstable, with large and abrupt changes in orientation. This is due partly to a faster winch speed during ascent. Frequent discharges of sediment from the piston corer may be due to vertical oscillations of the winch wire. The pilot corer would often hit the piston corer during ascent, also causing sediment discharges.

IV. PENETRATION, CORE SHORTENING AND CORE DISTURBANCES

Introduction

The lack of correlation between the recovered core length and the amount of penetration for cores collected by open-barreled gravity cores has been described by various workers (see, for example, Emery and Dietz, 1941). Following the development of the piston corer, the recovered length of core from a piston corer was often assumed to be equal to the corer's penetration into the bottom producing an undistorted core with no shortening (see, for example, Kullenberg, 1947; Ericson and Wollin, 1956; Ericson, et al., 1961). Evidence has been presented, however, to indicate that piston cores are indeed shortened (Hvorslev and Stetson, 1946; Kullenberg, 1955; Richards, 1961) and may have disturbed upper and lower sections (Ross and Riedel, 1967; Phillips, et al., 1968; Bouma and Boerma, 1968). Inderbitzen (1968), on the other hand, does not believe that shortening occurs in a Kullenberg piston core, but that it does destroy the surficial layer 75% of the time. Apparently both shortened and disturbed sections are a characteristic of the narrower diameter coring devices, such as the corer used in this study, but can be minimized by using larger diameter corers (Rosfelder and Marshall, 1967).

Core shortening is expressed as a percentage of the ratio between the length of core recovered and the amount of penetration by the corer into the bottom. If the actual amount of core shortening is to be determined, then the penetration must be accurately known. Indirect measurements of penetration have been made by measuring the amount of mud smeared along the outside of the core barrel (the mud-mark), by extrapolating the geothermal gradient to the sediment surface from heat flow measurements (Emery and Hulsemann, 1964), and by various other methods which reference the sediment surface to the core barrel.

Direct measurements of penetration were possible from the corehead camera photographs on 19 coring stations during CHAIN cruise 75, thereby allowing a more accurate determination to be made of core shortening for these cores and a comparison to be made with the more common indirect methods of determining penetration.

Intercomparisons between previous determinations of core shortening have been difficult because of the many variables involved in coring, such as the design of the corer (Emery and Dietz, 1941; Hvorslev and Stetson, 1946; Hvorslev, 1949; Kullenberg, 1955; Richards, 1961; Ross and Riedel, 1967), the type of corer (Emery and Dietz, 1941; Kullenberg, 1955; Richards, 1961; Emery and Hulsemann, 1964; Ross and Riedel, 1967), differing coring techniques at sea (Ross and Riedel, 1967), the character of the bottom sediments (Emery and Dietz, 1941), and the motions of the cable from which the equipment is suspended, especially in the case of piston corers (Kullenberg, 1955; Lister, 1964). Even where piston cores and open-barreled gravity cores have been taken simultaneously (the open barreled gravity corer being used as a pilot corer), the relationship of core shortening between the two types of corers has not been consistent; for example, Shepard (1963, figure 13), Ericson and Wollin (1956), and Emery and Hulsemann (1964) have described open-barreled gravity cores shortened relative to the piston cores whereas Ross and Riedel (1967) have described piston cores shortened relative to the open-barreled gravity cores. It may be significant that the open-barreled gravity corers used by both Ericson and Wollin (1956) and Emery and Hulsemann (1964) had a much smaller diameter than the accompanying piston corer, but that the open-barreled gravity corer used by Ross and Riedel had the same diameter as the piston corer. During CHAIN cruise 75, both the piston corer and the open-barreled pilot corer also had the same diameter.

It should be pointed out that the results reported here on core shortening as determined from the corehead camera photographs are strictly applicable only to the corer used during CHAIN cruise 75. Generally, however, these results are applicable to other piston corers and in a broad sense describe the efficiency of a piston corer in obtaining a representative sample of bottom sediment.

In piston coring, immobilization of the piston at the sediment surface is extremely critical if core shortening and core disturbances are to be reduced, and if a representative section of bottom-sediment is to be sampled. But, because of improper adjustment of the piston and/or incomplete penetration, cores obtained by piston corers frequently have missed or disturbed upper sections and sucked-in bottom sections. Core shortening in a piston core, in other words, may not result simply from thinning of the sedimentary column.

Measurement of Penetration

On the nineteen stations where good bottom photographs were obtained (given in Table IV), the depth of penetration was determined by measuring the width of the shadow cast by the bracket arm (mounted 1.5 m below the corehead) on the bottom and comparing it to the width of the bracket arm itself. To determine the shadow width with respect to varying distances below the corehead, the corer was rigged on land with two barrels, the cameras and strobe lights were mounted within the corehead (using the same cameras that were used at sea), and a large piece of cardboard was held at 30.5 cm (1 ft) intervals beneath the bracket arm to record the width of the shadow cast by the bracket arm. At least three pictures were taken at each interval. Figure 23 is one such picture taken by the camera focused at 1.8 m for penetration within 2.4 m (8 ft) of the corehead. Figures 24 and 25 are the calibration curves obtained from the camera focused at 1.8 m and the camera focused at 4.9 m. The deviation from a straight line is probably due to a broad light beam and diffraction effects around the edge of the bracket arm. By describing the measurement of the shadow width as a ratio of the width of the bracket arm, no correction was needed for print enlargement or for differences in refractive indices between lenses, water, and air to equate shadow widths on land with the shadow widths underwater. The deviations from vertical of the corer in the bottom did not significantly affect the measurements.

For the few stations where the bracket arm was buried, the coring barrel above the bracket arm was marked at 30.5 cm (1 ft) intervals during the calibration attempts. A transparent overlay showing these distances was then prepared and placed over the core barrels in the photographs, allowing the depth of penetration to be determined to the nearest 15 cm (6 in). The enlargement of the underwater photographs and the calibration photographs must be the same in this case.

Immobilization of the Piston

Precise adjustment of the amount of slack wire is absolutely necessary in piston coring if the piston is to be immobilized at the sediment surface and core shortening and disturbances are to be minimized. To properly determine the amount of slack wire needed, three important factors must be considered: (1) the distance of free-fall, (2) the strength of the sediments (Ross and Riedel, 1967), and (3) the contraction and elastic rebound of the cable after release of the heavy corer.

TABLE IV

Penetration, Length of Cores, Core Shortening, and Corer Orientations and Vertical Deviation in Bottom

Station No.	Photographically measured penetration* (cm)	Penetration suggested by mud mark(cm)	Penetration suggested by TG (cm)	Length of core recovered (cm)	Shortening ratio**	Corer Orientation on bottom (°)	Vertical Deviation of corer on bottom (°)	Remarks
2	850±10	850	--	328	.39	140	5	
4	--	870	--	468	--	--	---	no bottom plates
6	514±30	430	481±10	330	.64	310	8	
7	755±5	710	926	625	.83	300	10	
8	--	750	863±10	616	--	--	---	no bottom photos
9	--	925	--	792	--	--	---	no photos
10	--	425	431±50	525	--	--	---	corer bent
11	850±5	825	916±10	586	.69	290	10	
12	941+	940	926+	815	.86	--	---	part of core spilled on deck, corehead in mud
13	--	1296+	--	131	--	--	---	corer bent
14	758±5	725	808±15	760	1.00	230	10	
15	850±10	850	1036±10	790	.93	--	---	
16	741±10	650	636±10	378	.51	085	12	compass broken by pilot corer
17	880±5	800	--	44	.05	--	---	pretripped
18	865±10	865	876±10	860	.99	--	---	
19	--	250	--	143	--	--	---	no bottom photos
20	940	950	981±10	862	.92	--	---	corehead in mud
29	636+	---	621	488	.77	--	---	corehead in mud
30	636+	610	701±10	502	.79	--	---	corehead in mud
31	850±10	---	886±30	701	.83	240	10	
32	636±15	---	426±10	435	.68	220	16	
33	1296+	---	--	45	--	--	---	hit hard bottom and fell over
34	941+	914	--	900	.99	210	9	corehead in mud
35	941+	914	956±15	150	.16	135	12	pretripped, corehead in mud
36	941+	914	--	446	.47	--	---	corehead in mud
37	872±5	914	926±15	432	.50	--	---	
38	636±15	500	--	57	.09	140	11	pretripped
39	941+	953	1046±20	865	.92	--	---	corehead in mud
40	941+	914	1006±20	727	.77	--	---	corehead in mud
41	941+	991	--	9	.01	--	---	pretripped, corehead in mud
42	712±10	650	926±20	765	1.1	220	6	
43	850±20	850	--	696	.82	--	---	
44	683±15	650	--	837	1.2	335	5	
45	255±30	200	--	0	0	250	15	
45A	433±30	200	--	175	.40	225	8-18	
46	590±15	560	--	75	.13	--	---	

*Number followed by "+" indicates minimum penetration due to camera lenses being buried in bottom.

**Shortening ratio calculated by dividing the recovered core length by the photographically measured penetration.

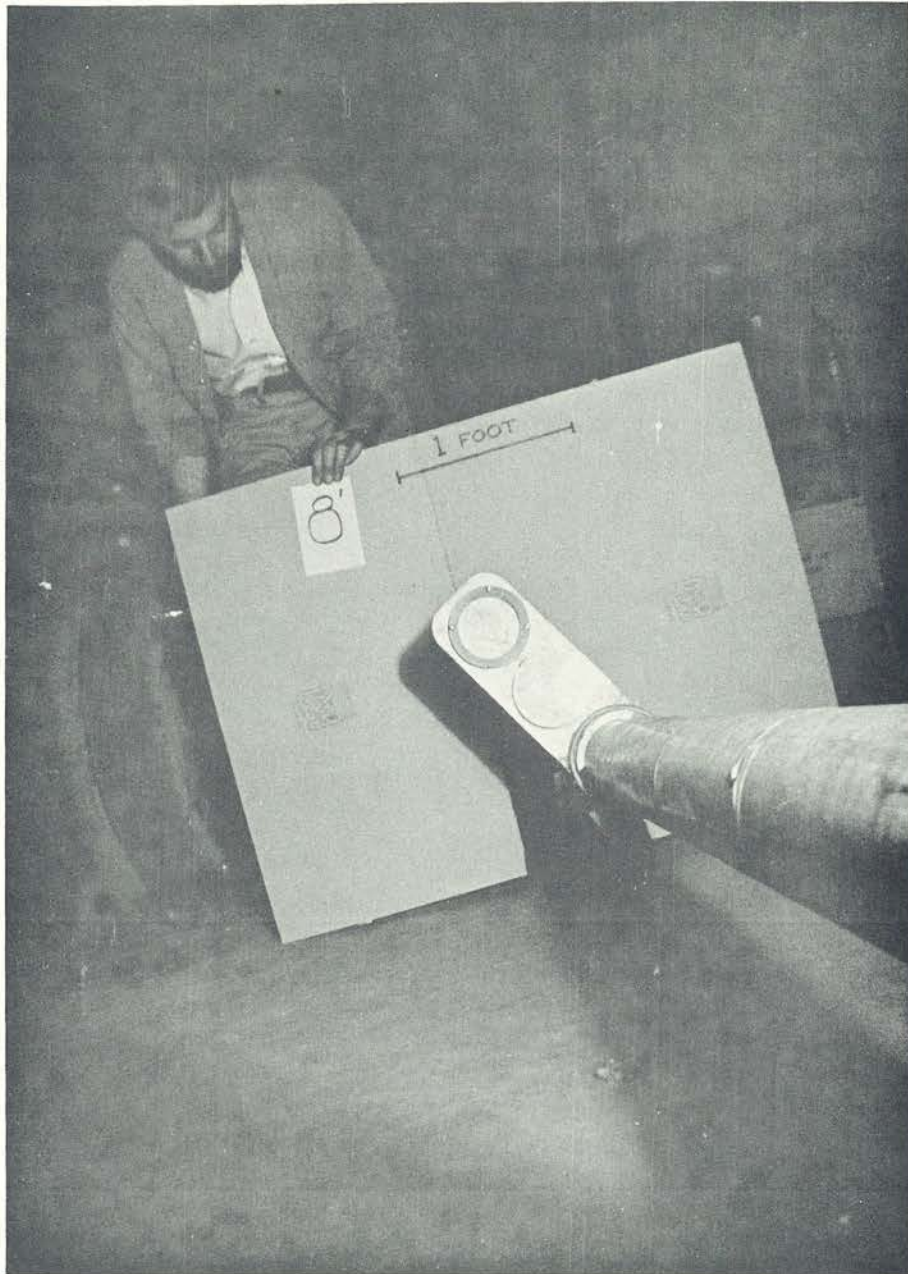


Figure 23. Calibration photograph used to determine the ratio of the bracket arm shadow width to the width of the bracket arm with penetration to within 8 ft of the base of the corehead. Photograph taken by the camera focused at 1.8 m (6 ft).

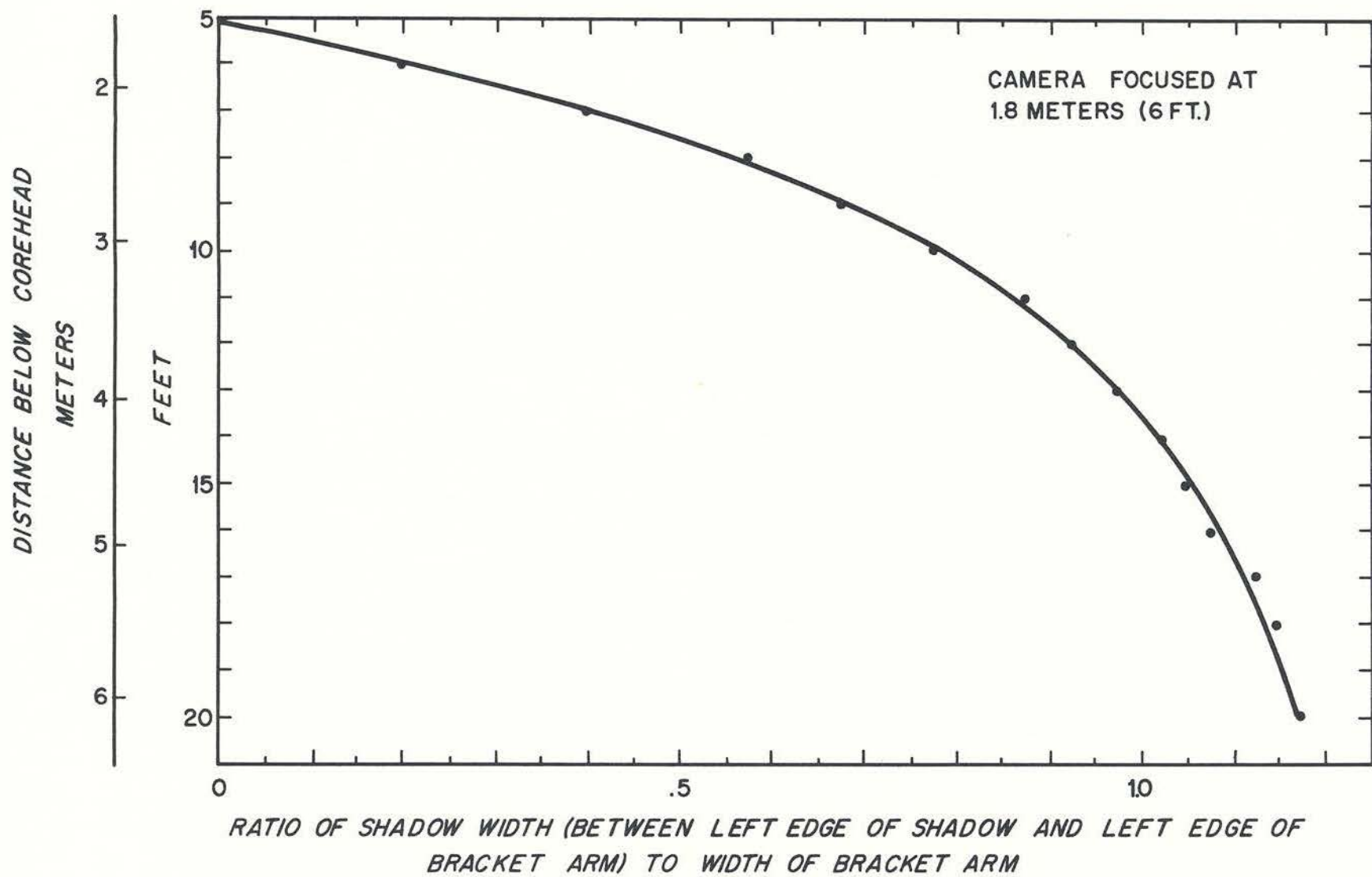


Figure 24. Calibration curve for the camera focused at 1.8 m (6 ft) to determine the amount of penetration as a function of the ratio between the width of the bracket arm shadow and the width of the bracket arm.

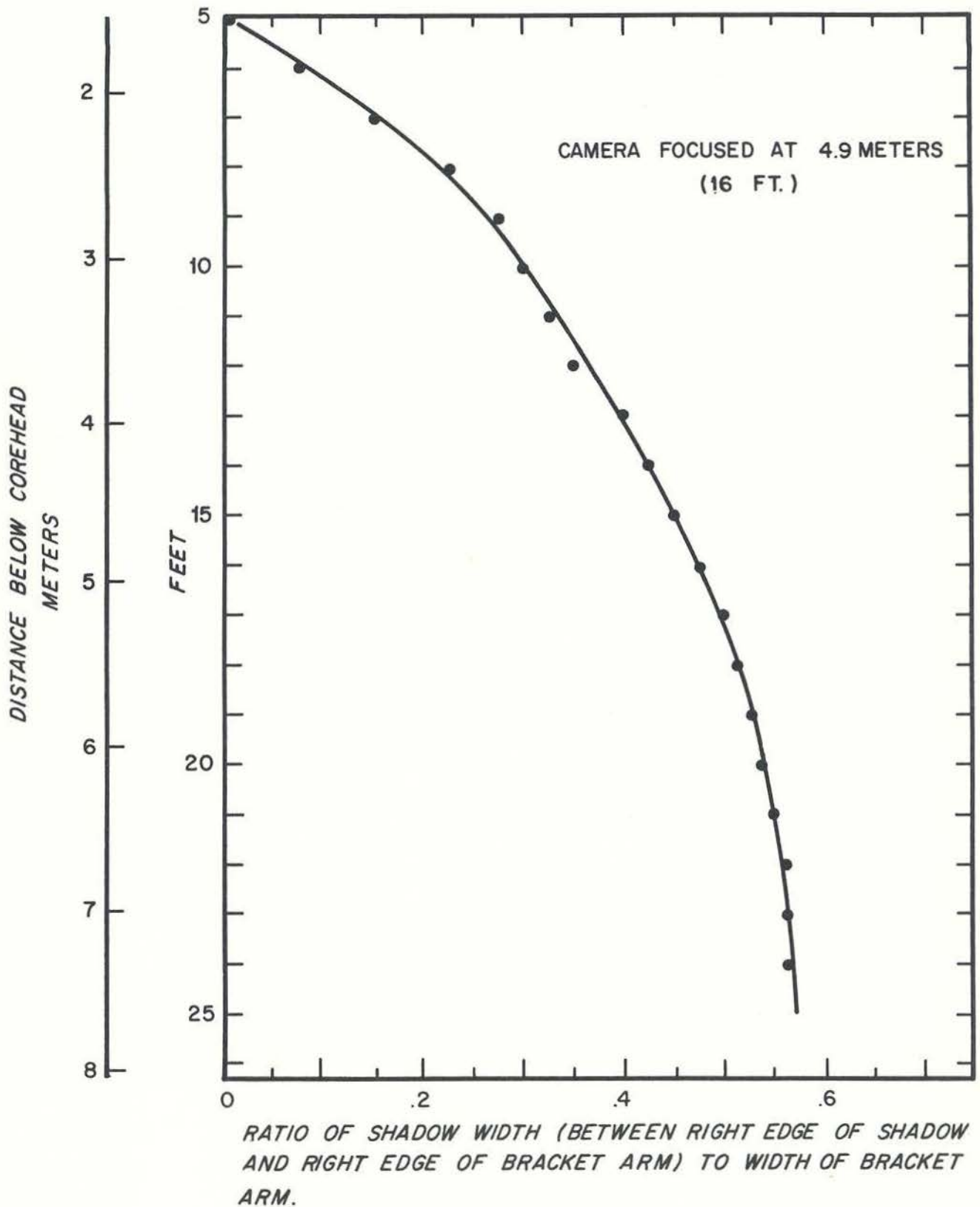


Figure 25. Calibration curve for the camera focused at 4.9 m (16 ft) to determine the amount of penetration as a function of the ratio between the width of the bracket arm shadow and the width of the bracket arm.

The distance of free-fall is, of course, the major adjustment; on CHAIN cruise 75 the distance was 6.7 m. An additional adjustment must be made for the distance that the tripping arm moves upwards before the piston corer is released.

The sediment strength will determine how far the pilot corer must penetrate before allowing the tripping arm to move upwards before releasing the piston corer (Ross and Riedel, 1967); this is a difficult adjustment to estimate, although it should be fairly constant for pelagic sediments.

The contraction and elastic rebound of the cable after the heavy piston corer is released represents a rather large and necessary adjustment. Cable contraction is a static response of the cable to the decrease in tension after the piston corer is tripped. Rebound, on the other hand, includes the dynamic response to the sudden decrease in tension when the piston corer is released, and may cause a greater amount of cable shortening than simple contraction. There may also be some elongation of the cable back to the static position after the dynamic response of rebound has diminished.

The cable used for coring operations was 1.27 cm (0.5 in) diameter, 3 x 19 steel cable manufactured by the U. S. Steel Corp., with a modulus of elasticity of 14.8×10^{11} dynes/cm (21.4×10^6 psi) and a breaking load of 12,300 kg (27,100 lbs). At the depths at which many coring operations are conducted, such as those during CHAIN cruise 75, great lengths (L) of cable must be used which, in turn, produces a significant amount of cable elongation or stretching. This change in length, ΔL_1 , due to the weight of the cable can be calculated by:

$$\Delta L_1 = \frac{wL^2}{2AE} \quad (\text{Rhodes, 1961})$$

where w = the weight per unit length (neglecting buoyancy), A = the cross-sectional area of the cable, and E = the modulus of elasticity. The weight of the piston corer, W , will produce an additional elongation of:

$$\Delta L_2 = \frac{WL}{AE} \quad (\text{Rhodes, 1961})$$

resulting in a total elongation ($\Delta L_1 + \Delta L_2$) of ΔL_T . Calculated values of cable elongation for various lengths of cable used during CHAIN cruise 75 are given in figure 26 for an unloaded and loaded cable. With the release of the piston corer near the bottom, the cable

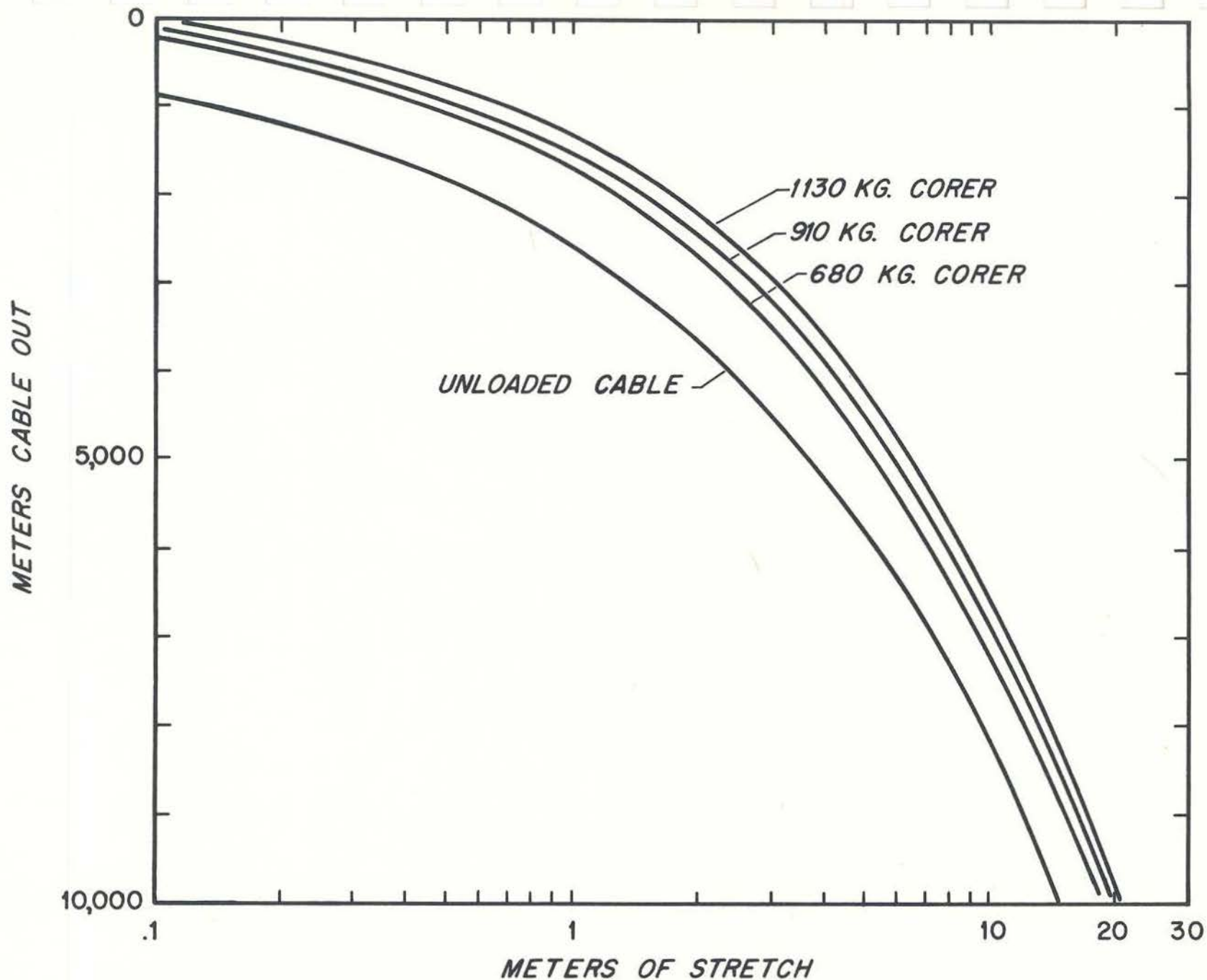


Figure 26. Amount of elongation, or stretch, of the cable used during coring operations on CHAIN cruise 75 with various lengths of cable out. Curves have been calculated for an unloaded cable (no corer attached) and for cables holding corers weighing 680 kg, 910 kg and 1130 kg.

will contract to its unloaded state; the total amount of contraction can be estimated from figure 26. For example, with 6,000 m of cable out, the cable will shorten from 9 m to 5.5 m after the release of a 1130 kg corer, or 3.5 m of contraction will occur.

The upwards displacement of the cable due to rebound can be determined by calculating the velocity of the elastic wave moving up the cable with time according to the relationship:

$$V = \frac{\Delta S}{A \sqrt{E\rho}} \quad (\text{Kullenberg, 1955}),$$

where A is the cross-sectional area of the cable, E is the modulus of elasticity of the cable, ρ is the average density of the cable, and ΔS is the tension discontinuity traveling upwards through the cable expressed as: $\Delta S = W - CX\phi$ (Kullenberg, 1955). Here, W is the weight of the corer, C the drag coefficient (given by Kullenberg as $0.037 \text{ gm}^2 / (\text{cm}^3)$), ϕ the diameter of the cable, and X the distance covered by the elastic wave during rebound. A plot of this relationship is shown in figure 27 as a function of the time from the moment of tripping and of the upwards distance traveled by the elastic wave, expressed as the amount of cable required to be added to the slack wire to compensate for rebound. The time of free-fall can be obtained from figure 8. Thus for the corer used during CHAIN cruise 75 with a free-fall distance of 6.7 m, approximately 1.6 m of extra cable must be added to compensate for rebound (figure 27) 1.3 seconds after tripping -- the time for free-fall (figure 8). Note that for depths greater than about 3,000 m, assuming no wire angle and a free-fall of 6.7 m in 1.3 seconds, cable rebound will be less than cable contraction and the additional slack wire needed will be the amount of cable contraction. At depths of less than about 3,000 m, however, with the same assumptions, cable rebound will exceed cable contraction and thus the needed additional slack wire will be the amount of cable rebound.

Unfortunately, even by careful adjustment of the slack wire other uncontrollable factors probably seriously affect the position of the piston. Vertical harmonic displacements of the corer while it is still attached to the end of the wire just prior to tripping may displace the piston by as much as 1.8 m or more once it is tripped (Lister, 1964). At the instant the corer is released, the winch must be stopped so that additional cable is not let out; this condition is difficult to achieve aboard ship. Any

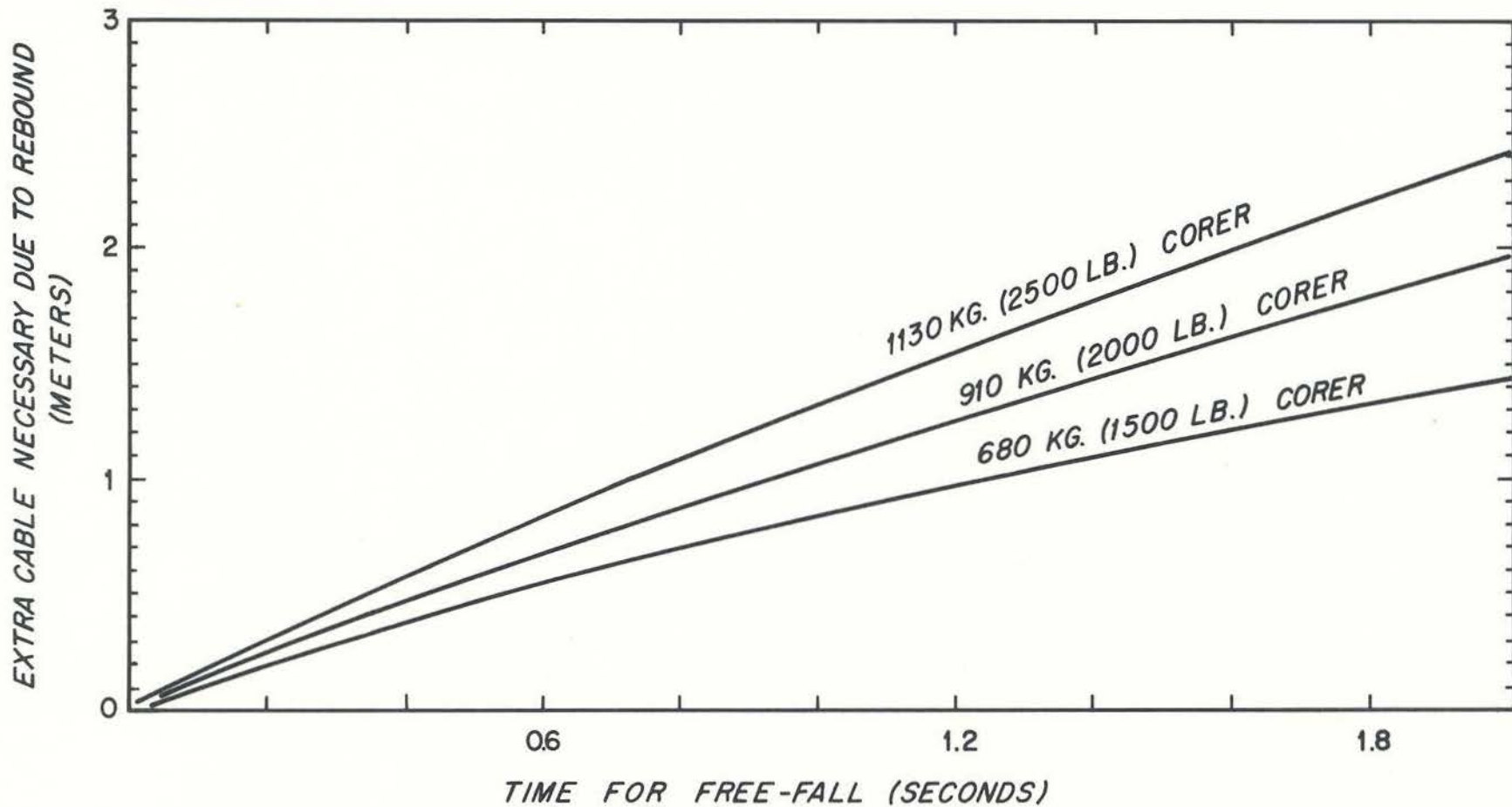


Figure 27. Extra cable necessary to compensate for elastic rebound of the cable after tripping of the piston corer, as a function of the time for free-fall.

additional cable let out will allow the piston to drop beneath the sediment surface. The piston, in fact, is probably already some distance beneath the sediment surface as the corer penetrates because of the increased downward pull on the piston due to internal friction within the core barrels. If the slack wire is taped too securely to the tripping arm, the tape may not break instantly thereby causing the piston to move upwards in the barrel during free-fall. On the other hand, if the taping is not done strongly enough, the slack wire will break loose during descent, as for example, occurred frequently during ATLANTIS II cruise 42, increasing the possibility of losing the corer should this wire become tangled around the piston corer. Because of these additional difficulties, Kullenberg (1955) has aptly pointed out that "it is not possible to immobilize the piston completely at a great depth".

Relationship Between the Core Recovered and Penetration

No clear relationship was noticed on the CHAIN cruise 75 cores between the photographically measured penetration and the length of core recovered, as is evident from figure 28 and Table IV. On the 15 stations where penetration could be accurately measured in the photographs, the average core recovery was 76%, but with a wide variation. Figure 28 includes these 15 stations, with seven additional stations plotted. Photographs from six of the latter seven stations (stations 29, 30, 34, 36, 39 and 40) indicated maximum penetration by the camera lenses being buried in the bottom.

No relationship between the general sediment type and either the length of core recovered or the penetration seems to be apparent in figure 28.

Interestingly, on stations 42 and 44 the photographically measured penetration was less than the core recovered, yet neither core showed evidence of sucked-in lower sections. This might imply that a significant portion of the core was sucked-in but without the usual blurring or destruction of layering in the lower portion of the core. Artificial stratification that has been produced by a piston moving upwards has been described in cores taken by small piston corers in laboratory experiments (Burns, 1963). A similar situation might also develop if the piston were to move upwards at a faster rate than the rate of penetration, producing, in this case, either false stratification or unnaturally thicker individual layers.

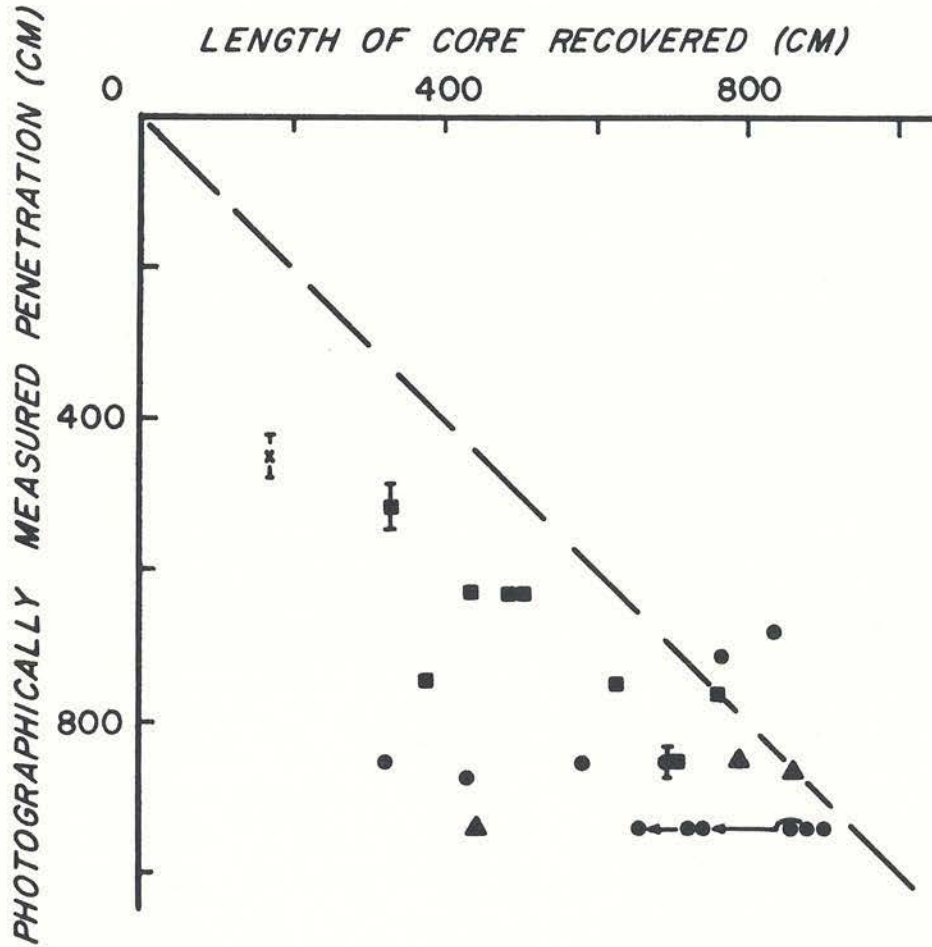


Figure 28. Relationship between the photographically measured penetration and the length of core recovered. Symbols represent: squares - sediment in core predominately calcareous ooze; circles - sediment in core predominately "red mud"; triangles - sediment in core both calcareous ooze and "red mud"; "X" - sediment in core entirely a sandy silt; arrows - correction of core length by subtraction of "sucked in" material at bottom of core; brackets denote range of error in determining penetration from photographs; dashed line represents 100% core recovery (no shortening).

Comparison of Pilot Cores and Piston Cores

Comparison between a corresponding pair of piston and pilot cores indicate that on the majority of the stations nearly the entire sequence cored by the pilot corer is missing from the adjacent piston core. For example, the piston core taken on station 45A contains a thick sandy silt sequence (F. S. Birch, personal communication) that is not found in the 145 cm pilot core. Direct comparisons are possible on cores from only a few stations; in these cases, thinner laminae, distorted and bent contacts between laminae, and sharper contacts between layers suggest that the piston core has been both shortened and disturbed as compared to the adjacent pilot core collected with an open-barreled gravity corer. For these few stations where a correlation can be made on the basis of distinct horizons or sequences, the piston core has been shortened by as much as a factor of 4.5 relative to the pilot core. This degree of relative shortening and loss of the upper portion of the piston core agrees with descriptions by Ross and Riedel (1967), Phillips, et al., (1968) and Inderbitzen (1968). Without detailed mineralogical and paleontological investigations on each pair of cores, more specific correlations are not possible.

Core Shortening

Although the average core recovery was 76% (shortening ratio of .76), a considerable variation in the shortening ratio occurred from station to station (Table IV). The excess or deficiency of slack wire used or the general sediment type did not noticeably affect the amount of core shortening. It should be pointed out that a measurement of core shortening as a ratio of the recovered length of core to the length of penetration assumes 100% core recovery unless sucked-in lower portions can be identified and subtracted. But the difficulties described in retaining the piston at the sediment surface, and the comparisons made between piston and pilot cores clearly indicate that the upper portion of the piston core is frequently lost during the coring process; thus the lack of a clear relationship between core shortening and the excess or deficiency of slack wire used is not surprising. Rather, the shortening ratio is probably a function of the corer's design (Ross and Riedel, 1967).

The deviation of the corer from vertical in the bottom did not seem to noticeably influence the shortening ratio.

Relationship Between the Mud-Mark and Penetration

One of the most frequently used methods for determining penetration is to measure the distance to the upper level of smeared mud along the outside of the core barrel. Figure 29 shows the relationship between the position of the mud-mark and the photographically measured penetration for 23 stations during CHAIN cruise 75 (see also Table IV). The mud-mark for most of these stations averaged about 30 cm less than the actual penetration, with only a small variation. This slight difference may, in fact, represent the actual upper contact between the core barrel and the bottom sediment, considering the depressions and widened holes noticed in the bottom photographs on many stations (see figures 16 and 17). On five stations the mud mark was exactly the same as the measured penetration, and only three stations recorded mud-marks higher than the penetration. The determination of the mud-mark position was always made by an experienced group during the CHAIN cruise; only these determinations are plotted in figure 29. Other independent determinations made during the cruise differed considerably. The general sediment type did not seem to effect the position of the mud-mark (figure 29). Thus it appears that the position of the mud-mark is an accurate and reliable indicator of penetration.

Relationship Between the Geothermal Gradient and Penetration

Heat flow measurements taken by thermistors attached along the exterior of the core barrels (Gerard, et al., 1962) provide another method of estimating penetration by extrapolation of the geothermal gradient to the sediment surface (see, for example, Emery and Hulsemann, 1964). The relationship of this implied penetration to the photographically measured penetration is shown in figure 30. On the average, the penetration indicated by the geothermal gradient was about 60 cm greater than the actual penetration, but with a wide variation (Table IV). Geothermal gradients in red muds seemed to give a slightly higher implied penetration than calcareous oozes, although without more data this can only be considered a tentative suggestion. Thermal conductivities and relative water contents calculated from Ratcliffe (1960) did not vary significantly between the two sediment types in the CHAIN 75 cores. Thus the generally higher and wider variation in implied penetration from heat flow data may be due to a nonlinear geothermal gradient near the surface of sediment. Bottom water temperature fluctuations could account for nonlinear geothermal gradients near the sediment surface. Lubimova, et al., (1965) have

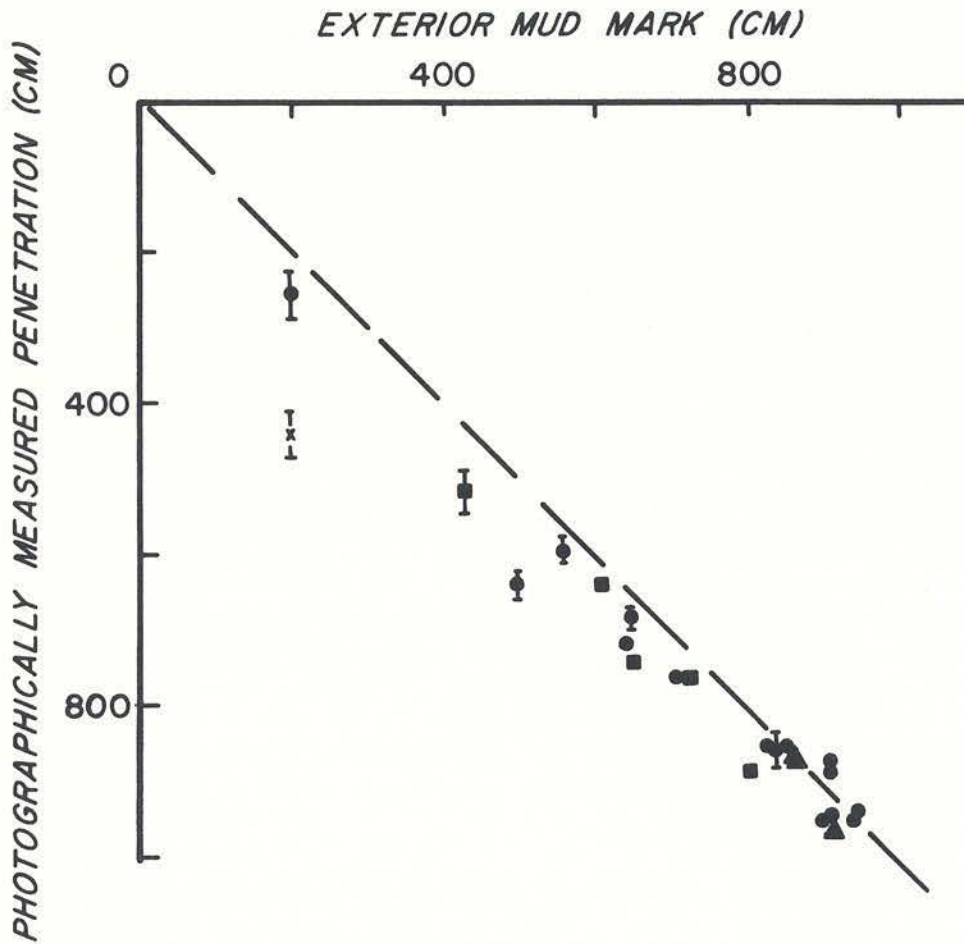


Figure 29. Relationship between the position of the exterior mud-mark and the photographically measured penetration. See figure 28 for an explanation of the symbols.

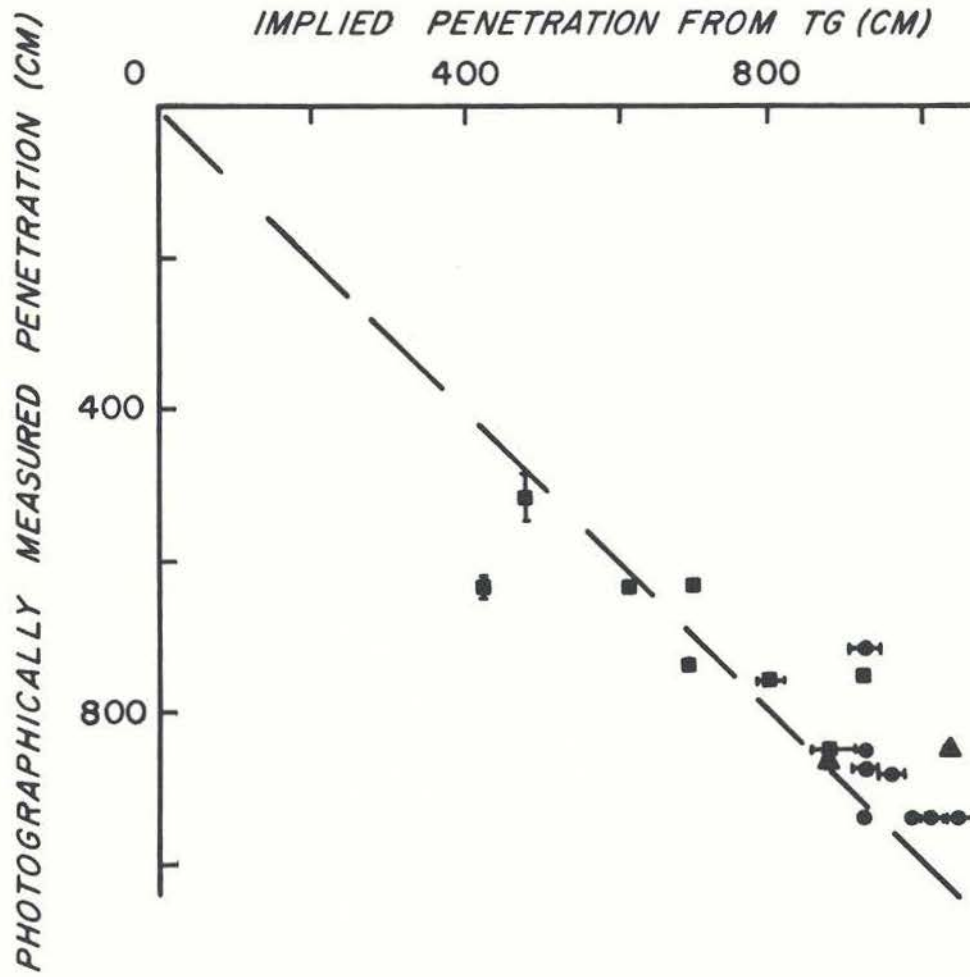


Figure 30. The relationship between the implied penetration as extrapolated from the thermal gradient (TG) and the photographically measured penetration. See figure 28 for an explanation of the symbols.

described slight increases in water temperature within 50 to 3 m of the bottom, although Langseth, et al., (1966) did not find such a water structure over the Mid-Atlantic Ridge. Bottom currents may also locally vary the lower water temperature structure (Lubimova, et al., 1965). For example, the colder, northward flowing Antarctic Bottom Water, which was encountered on some of the stations during the CHAIN cruise (McCoy, 1969), has been reported to have a noticeable effect on the geothermal gradient on other stations (Gerard, et al., 1962; Langseth, et al., 1966). Either of these variations in the temperature structure of the water near the sediment surface might produce the slightly higher implied penetration suggested by the geothermal gradient.

Relationship Between the Vertical Deviation of the Corer in the Bottom and Penetration

Within the 0-18° angle detection limits of the inclinometer, the deviation from vertical of the corer in the bottom apparently had no effect on the amount of penetration (Table IV). During penetration, the deviation of the corer increased by an average of 6° (see Section III), but this also did not appear to influence the amount of penetration.

Relationship Between Stratigraphic Dips in the Cores and the Vertical Deviation of the Corer in the Bottom

On the 15 stations where the vertical deviation of the corer in the bottom was photographically recorded (Table IV), the average stratigraphic dip within the recovered core reflected this vertical deviation on only one station. In this one case, the stratigraphic dip was half the 10° vertical deviation recorded by the inclinometer. Stratigraphic dips varied considerably within a single core, rarely reflecting the corer's deviation from vertical in the bottom and probably even more rarely reflecting in situ dips. Apparently, these dips preserved in the piston cores have been largely produced during the coring process.

This lack of correlation of bedding dip with the attitude of the coring apparatus in the bottom may produce some bias in bottom thermal gradient and heat-flow measurements. The assumption has been made for many measurements made by the Ewing method of thermal probes attached to a core barrel (Gerard, et al., 1962) that horizontal layers in a core are an

indication of near-vertical penetration, but our measurements indicate that this may not be reliable. The error is simply in the ratio of the cosine of the angular deviation from vertical, and becomes significant for deviations greater than about 15°.

Summary

Accurate determinations of the amount of penetration were possible from the corehead camera bottom photographs on 19 stations. This, in turn, allowed comparisons to be made with the length of core recovered and with other common methods of indirectly measuring a corer's penetration, such as the position of the mud-mark and the extrapolation of the geothermal gradient to the sediment surface from heat-flow measurements.

No consistent relationship was found between the length of core recovered and the amount of penetration. The amount of core shortening, then, varied considerably with an average shortening of .76. Core shortening does not seem to be a function of an excess or deficiency of slack wire or the corer's deviation from vertical in the bottom. Comparisons between piston and pilot cores indicated that the piston cores had been shortened and disturbed relative to the pilot cores, and that as much as a meter of the upper portion in the piston core has been lost. This loss of the upper section probably results from the near-impossibility of immobilizing the piston at the sediment surface.

The position of the mud-mark appears to be a very reliable indicator of penetration, providing the measurement is made by a person experienced in its determination. Extrapolation of the thermal gradient to the surface of the sediment from heat-flow measurements is less reliable.

The vertical deviation of the corer in the bottom does not influence the amount of penetration. Stratigraphic dips in the recovered cores apparently result from disturbances during penetration; they correspond poorly to the corer's vertical deviation in the bottom.

V. BOTTOM CURRENT MEASUREMENTS

The recognition and measurement of possible bottom currents in corehead camera bottom photographs has been reported elsewhere (McCoy, 1969), but shall be described here as an example of additional information that can be obtained from these photographs.

Bottom currents in the CHAIN 75 photographs could be distinguished in three ways; (1) as a narrow streaming sediment cloud issuing from around the base of the core barrel as the corer rested in the bottom (figures 16 and 31); (2) as a slowly moving diffuse, higher cloud of sediment that frequently obscured the bottom (figure 32); or (3) by the pronounced asymmetry of the initial sediment cloud raised when the corer entered the bottom.

The best indication of bottom currents was the narrow, streaming sediment cloud which usually continued throughout a station, about five minutes, moving very near the bottom with distinct boundaries. Its direction of movement varied only $\pm 8^\circ$ for all stations at which it was present, with a maximum variation of 14° . The diffuse sediment cloud, slowly moving in a consistent direction, appeared slightly higher off the bottom and may have been initiated outside of the field of view by the pilot corer. Directions could not be as accurately determined for this type of cloud. In the CHAIN 75 bottom photographs, these sediment clouds were not seen simultaneously with the narrow, streaming sediment cloud, perhaps because the more diffuse cloud masked the bottom; however, both types of sediment clouds were noticed together in the corehead photographs of a few stations during ATLANTIS II cruise 42 and indicated the same general direction for bottom currents. Asymmetrical dispersion of the initial sediment cloud produced by the piston corer entering the bottom also indicated a general direction for bottom currents. In a few cases a narrow, streaming sediment cloud issued from around the core barrel after an asymmetrical cloud was produced; both indicated bottom currents in the same direction. The asymmetry did not appear to be related to the deviation from vertical of the corer during penetration. A small vane was mounted on the end of the bracket arm during a few coring stations on CHAIN cruise 82; and indicated bottom currents flowing in the same direction as that suggested by the sediment clouds (P. Leonard, personal communication).

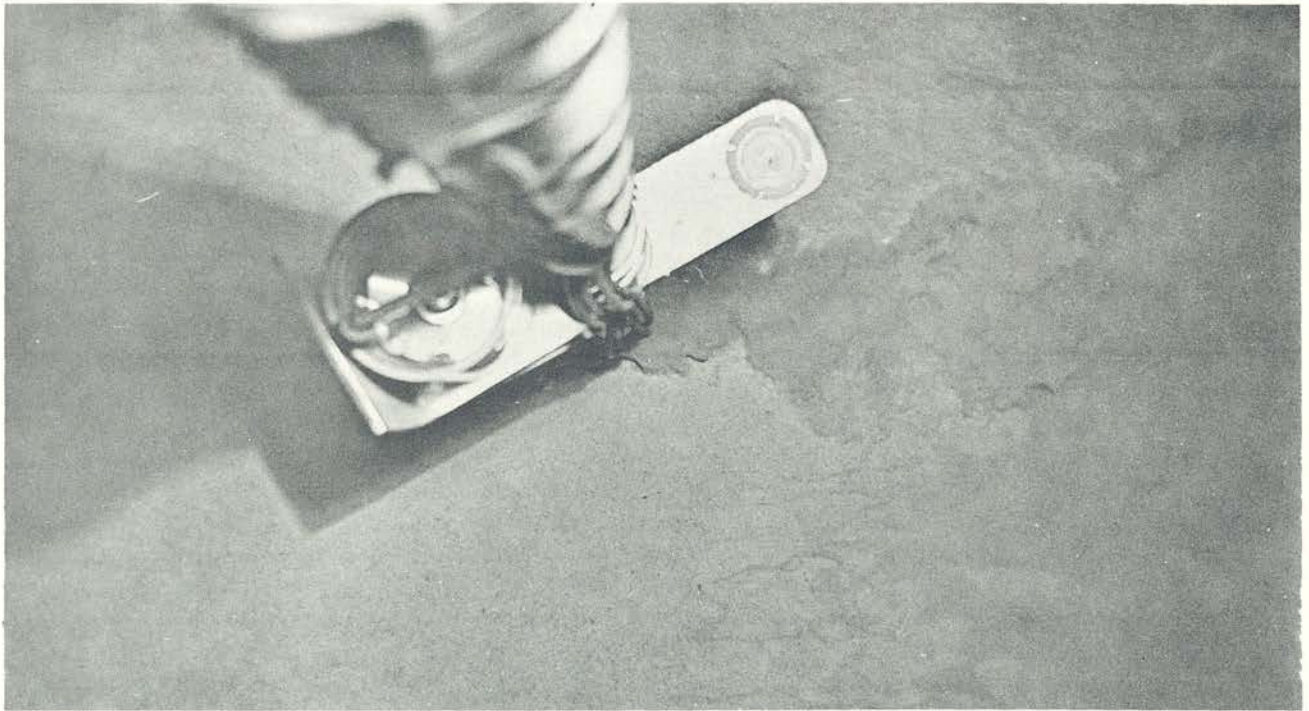


Figure 31. Bottom currents producing a narrow streaming sediment cloud around the base of the core barrel during station 16. Note smaller sediment clouds on the sea floor near the corer. Photograph taken by the camera focused at 4.9 m (16 ft).

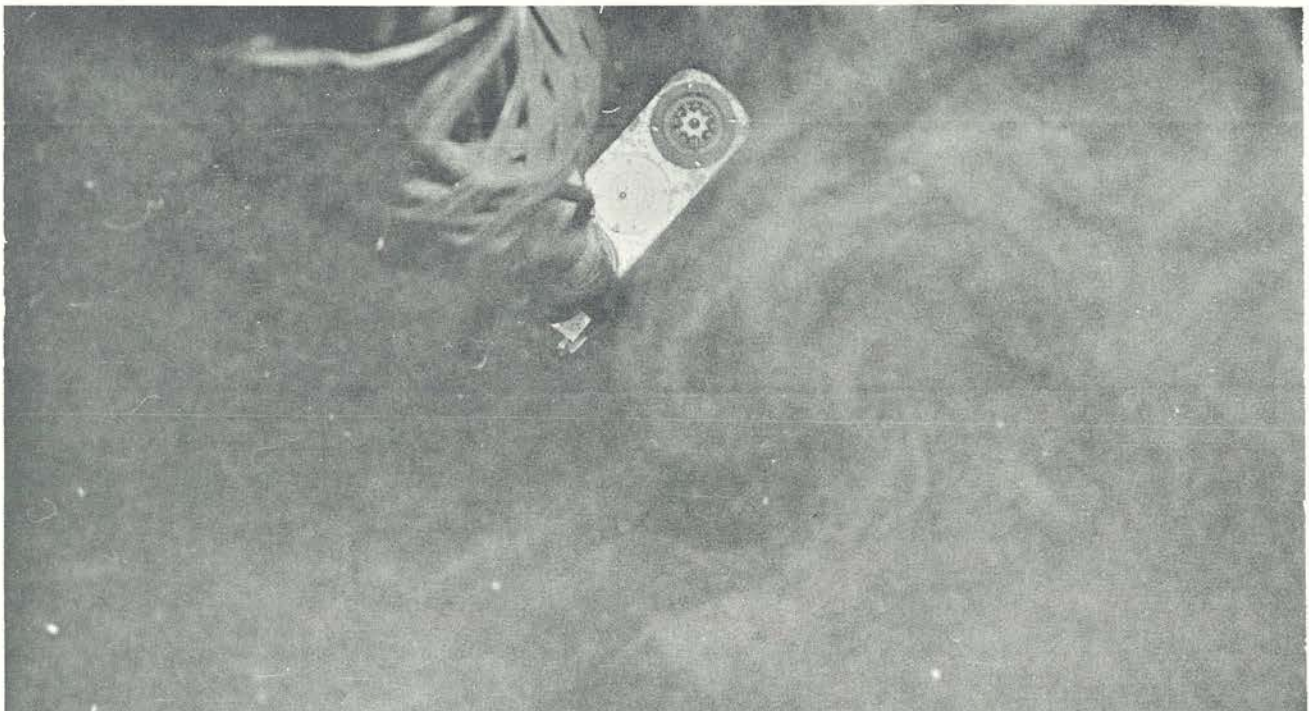


Figure 32. Higher, diffuse sediment cloud during station 44 moving in response to bottom currents. Photograph taken by the camera focused at 4.9 m (16 ft)

Approximate velocities for the bottom currents were estimated from the photos by timing the advance of a particularly obvious portion of the turbulent sediment cloud. During the few stations on CHAIN cruise 75 where estimates could be made, the velocities varied from 1-3 cm/sec. Relative magnitudes for velocities were also made on the basis of the time required for the dispersion of the initial sediment cloud.

Bottom current evidence was recorded on 19 stations during CHAIN cruise 75. The majority of these bottom currents had a southerly direction except near the Lesser Antilles Island Arc and on the Mid-Atlantic Ridge (figure 33), suggesting a continuation of the Western Boundary Undercurrent (Heezen, et al., 1966; Schneider, et al., 1967) over the Western Guiana Basin to at least 12°N latitude. Further experiments will be conducted on future lowerings to determine if the currents do persist higher above the bottom; current meters hopefully can be mounted within the corehead for more accurate measurements.

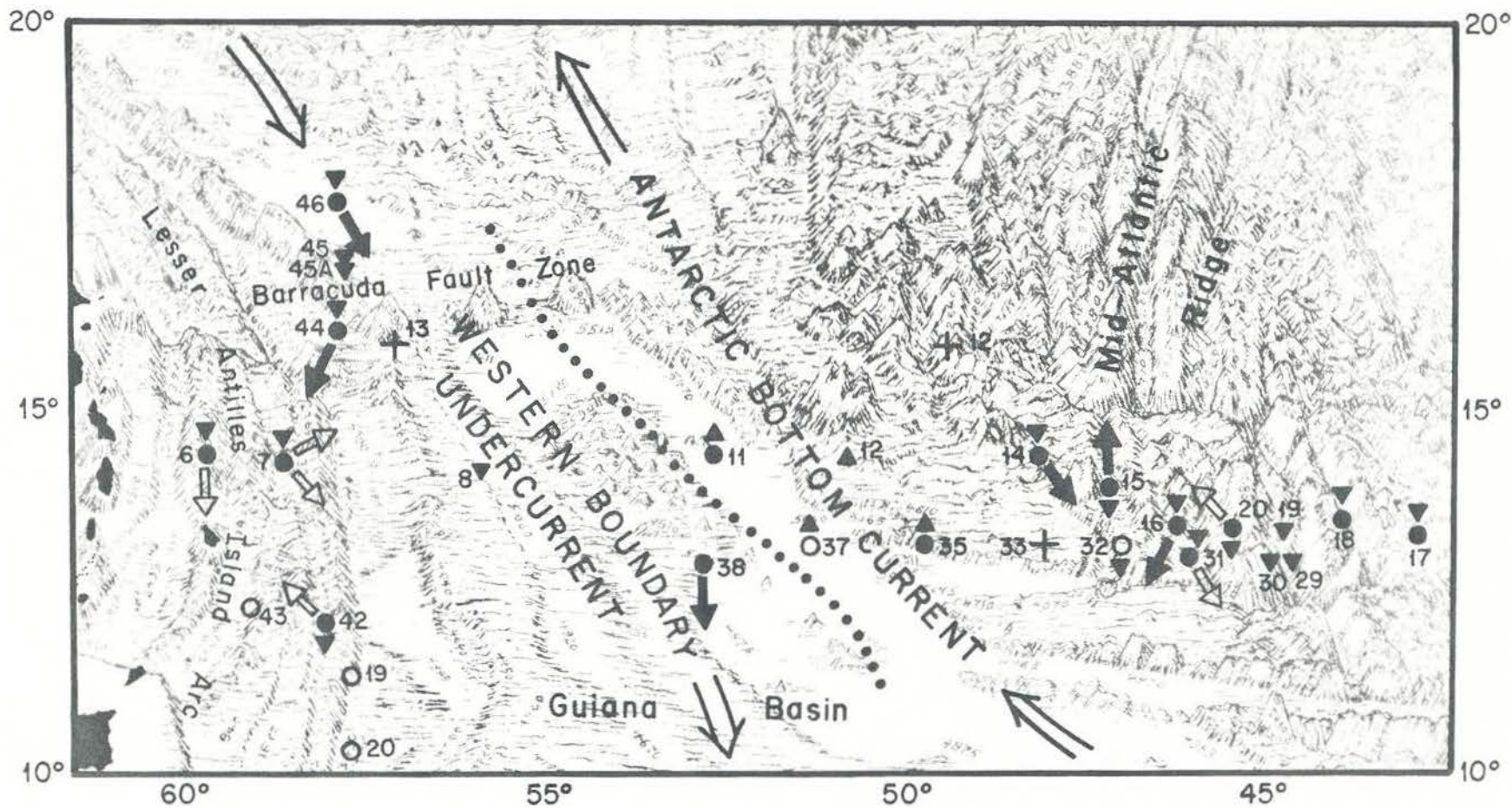


Figure 33. Bottom current directions between the Lesser Antilles and the Mid-Atlantic Ridge (McCoy, 1969). Solid arrows indicate bottom current directions observed at depths greater than 3600 m. Open arrows indicate bottom current directions observed at depths less than 3600 m. Solid circles indicate stations where bottom currents observed but direction not determinable. Crosses indicate stations where bottom features seen in photographs suggest the presence of bottom currents. Open circles indicate stations showing tranquil conditions in bottom photographs. Triangles indicate *in situ* bottom temperatures: for temperatures of less than 2°C apices point north, for temperatures greater than 2°C apices point south. Numbers beside symbols are station numbers. The dotted line represents the approximate inferred boundary between the northward flowing, colder Antarctic Bottom Current and the southward flowing, warmer Western Boundary Undercurrent. This is a portion of the Physiographic Diagram of the South Atlantic Ocean, published by the Geological Society of America. Copyright © 1961 Bruce C. Heezen and Marie Tharp. Reproduced by permission.

VI. RECOMMENDATIONS FOR FUTURE PISTON CORING

Certain recommendations or suggestions to be used in future piston coring programs arise from this analysis of corehead camera photographs and from the examination of the cores recovered.

Vertical oscillations of the cable largely destroy the necessary requirement of piston coring - the effective immobilization of the piston at the sediment surface. If these oscillations are to be dampened, then constant tension winches must be used (Lister, 1964). Only then can other factors such as cable stretching, cable rebound, and the time lag between tripping and stopping of the winch be considered and effectively accounted for.

If possible piston coring should always be conducted with an open-barreled gravity corer as the pilot corer. This is necessary if any of the upper portion of the sediment column is to be sampled.

If piston coring is continued using narrow-diameter core barrels, with their apparent distortion of the sample, then either piston arrestors or pistons which can be deactivated should be used. Piston arrestors so far are unsatisfactory when used with liners. Kullenberg (1955) used a two-piece, disconnecting piston that required a decrease in cable tension for activation. Fleming and Calvert (no date) and Woodruff (1967) have described hydraulic devices that release the cable from the piston when tripping occurs, thereby preventing the piston from being raised within the core barrel during pull-out and eliminating sucked-in lower portions of the core. Kermabon and Cortis (1968) have devised a recoilless piston linked by exterior pulleys to a large exterior plate that remains at the sediment surface. All of these methods isolate the piston from the cable so that any increase in cable tension does not raise the piston. The device described by Kermabon and Cortis (1968) will prevent the piston from being affected by vertical oscillations of the cable; an additional advantage of this design might be that the exterior pulley mountings would act as stabilizing fins in the bottom. The use of any of these piston deactivators is recommended over the presently used system.

One-way check-valves in the pistons would allow trapped water to escape during penetration, decreasing the lateral displacement of water and increasing the chance for recovering some of the surface sediment in the piston core.

The position of the mud-mark has been shown to be a very effective indicator of the amount of penetration. For future operations where core-head cameras might not be used and penetration cannot be directly measured, a thin band of grease up the core barrels might help to even more accurately define the mud-mark (Emery and Dietz, 1941).

Rotation of the corer during free-fall and penetration, causing differential rotation of the liners, might be partially prevented by using a swivel above the piston; this, however, might cause difficulties when the piston is brought up against the piston-stop within the corer.

Although Burns (1966) believes fins are necessary for stabilization of a corer during free-fall, corehead camera photographs indicate that the corers used in this study accomplish free-fall with only a small increase in vertical deviation.

The presently used camera settings, both in focus distance and in aperture settings, seem to be adequate. Unfortunately the cameras and/or the compass-inclinometer are frequently buried in the bottom.

The compass and inclinometer also seem to work very well. Compasses with large, clear north-arrows should be used whenever possible so that orientations can be read in the photographs taken by both cameras.

Current meters hopefully can be placed within the corehead in the future to accurately measure bottom currents.

Perhaps longer tripping arms will prevent the pilot corer from penetrating so close to the piston corer. From the photographs it is obvious that an improved pilot corer must be developed and some method devised to keep it from being withdrawn prematurely because of increases in cable tension.

REFERENCES

- Bouma, A. H. and J. A. K. Boerma, 1968, Vertical disturbances in piston cores, *Marine Geology*, 6, 231-241.
- Burns, R. E., 1963, A note on some possible misinformation from cores obtained by piston-type coring devices, *J. Sed. Pet.*, 33, 950-952.
- Burns, R. E., 1968, Free-fall behavior of small, light-weight gravity corers, *Marine Geology*, 4, 1-9.
- Edgerton, H. E., 1967, The instruments of deep-sea photography, *in* Hersey, ed: *Deep-Sea Photography*, Johns Hopkins Press, 47-54.
- Emery, K. O. and R. S. Dietz, 1941, Gravity coring instrument and mechanics of sediment coring, *Bull. Geol. Soc. Am.*, 52, 1685-1714.
- Emery, K. O. and J. Hulsemann, 1964, Shortening of sediment cores collected in open barrel gravity corers, *Sedimentology*, 3, 144-154.
- Ericson, D. B. and G. Wollin, 1956, Correlation of six cores from the equatorial Atlantic and the Caribbean, *Deep-Sea Res.*, 3, 104-125.
- Ericson, D. B., M. Ewing, G. Wollin, and B. C. Heezen, 1961, Atlantic deep-sea cores, *Bull. Geol. Soc. Am.*, 72, 192-286.
- Ewing, M., D. E. Hayes and M. Thorndike, 1967, Corehead camera for measurement of currents and core orientation, *Deep-Sea Res.*, 14, 253-258.
- Fleming, C. S. and S. E. Calvert, no date, The piston immobilizer: a further modification to the piston corer, *Scripps Inst. of Ocean. Tech. Report*, no number given, 10 pp.
- Gerard, R., M. G. Langseth and M. Ewing, 1962, Thermal gradient measurements in the water and bottom sediment of the western Atlantic, *J. Geophys. Res.*, 67, 785-803.

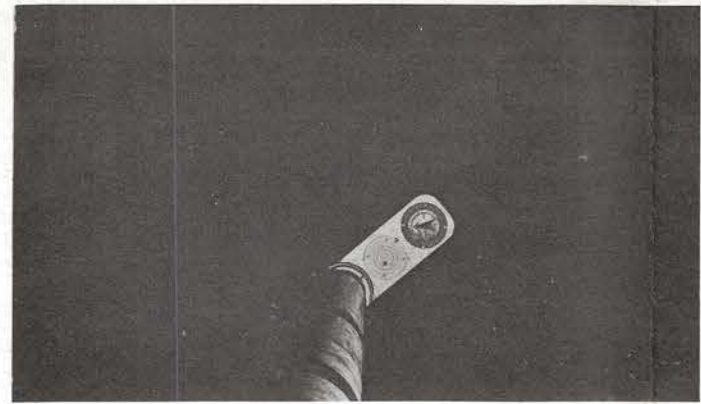
- Heezen, B. C., C. D. Hollister and W. F. Ruddiman, 1966, Shaping of the continental rise by deep geostrophic contour currents, *Science*, 152, 502-503.
- Hopkins, R. E. and H. E. Edgerton, 1961, Lenses for underwater photography, *Deep-Sea Res.*, 8, 312-316.
- Hvorslev, M. J., 1949, Subsurface exploration and sampling of soils for civil engineering purposes, *Tech. Rep. U. S. Corps Engrs. Waterways Expt. Sta.*, 521 pp.
- Hvorslev, M. J. and H. C. Stetson, 1946, Free-fall coring tube: A new type of gravity bottom sampler, *Bull. Geol. Soc. Am.*, 57, 935-950.
- Inderbitzen, A. L., 1968, A study of the effects of various core samples on mass physical properties in marine sediments, *J. Sed. Pet.*, 38, 473-489.
- Kermabon, A. and U. Cortis, 1968, A recoilless piston for the SACLANTCEN sphincter corer, *SACLANTCEN Tech. Report No. 112*, 25 pp.
- Kullenberg, B., 1947, The piston core sampler, *Sv. Hydro. - Biol. komm. Skv., Tredje Ser. Hydr.*, 1, 1-46.
- Kullenberg, B., 1955, Deep-sea coring, *Rep. Swed. Deep-Sea Exped.*, 4, 35-96.
- Langseth, M. G., X. LePichon and M. Ewing, 1966, Crustal structure of the mid-ocean ridges, 5. Heat flow through the Atlantic Ocean floor and convection currents, *J. Geophys. Res.*, 71, 5321-5355.
- Lister, C. R. B., 1964, On the vertical motion of equipment lowered by wire into the deep-sea, *Bull. Institutului Politehnic din Iasi*, 10, (14), 87-96.
- Lubimova, E. A., R. P. Von Herzen and G. B. Udintsev, 1965, On heat transfer through the ocean floor, in: *Terrestrial Heat Flow*, A. G. U. Mono. No. 8, 78-86.

- McCoy, F. W., Jr., 1969, Bottom currents in the western Atlantic Ocean between the Lesser Antilles and the Mid-Atlantic Ridge, *Deep-Sea Res.*, 16(2), 179-184.
- Phillips, J. D., W. A. Berggren, A. Bertels and D. Wall, 1968, Paleomagnetic stratigraphy and micropaleontology of three deep sea cores from the central North Atlantic Ocean, *Earth and Planetary Science Letters*, 4, 118-130.
- Ratcliffe, E. H., 1960, The thermal conductivities of ocean sediments, *J. Geophys. Res.*, 65, 1535-1541.
- Rhodes, R. S., 1961, unpublished manuscript, Woods Hole Oceanographic Institution, 8 p.
- Richards, A. F., 1961, Investigations of deep-sea sediment cores, I. Shear strength, bearing capacity and consolidation, U. S. Navy Hydrographic Office Tech. Rept. 63, 70 pp.
- Rosfelder, A. M. and N. F. Marshall, 1967, Obtaining large, undisturbed, and oriented samples in deep water, *in* Richards, ed.: *Marine Geotechnique*, Univ. of Illinois Press, 243-263.
- Ross, D. A. and W. R. Riedel, 1967, Comparison of upper parts of some piston cores with simultaneously collected open-barrel cores, *Deep-Sea Res.*, 14, 285-294.
- Schneider, E. D., P. J. Fox, C. D. Hollister, H. D. Needham and B. C. Heezen, 1967, Further evidence of contour currents in the western North Atlantic, *Earth and Planetary Sci. Letters*, 2, 351-359.
- Shepard, F. P., 1963, *Submarine Geology*, 2nd ed., Harper and Row, New York, 557 pp.
- Woodruff, J. L., 1967, A device for releasing a piston corer and deactivating the piston, *Deep-Sea Res.*, 14, 809-819.

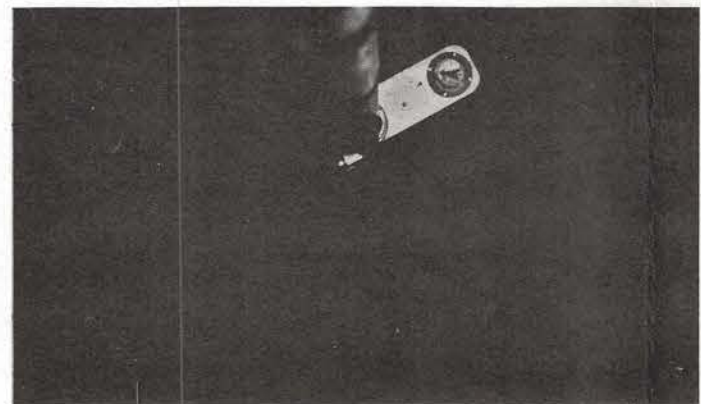
PLATE I

Sequence of photographs taken by both cameras during coring operations on station 7, CHAIN cruise 75. Pictures arranged horizontally in time sequence, with approximately 5 sec between successive pictures, except where time interval is noted. Beginning at upper left, the sequence shows: (1) immediately prior to tripping, (2) during penetration, which was completed in about 5 sec, (3) and (4) following complete penetration. The next pair of pictures (upper right) were taken about one minute later while the corer was in the bottom - note streaming sediment cloud produced by bottom currents. Pull-out is shown at lower left (bottom two rows), complete withdrawal from the bottom taking about 15 sec. During ascent (lower right), the pilot corer repeatedly swung into view, and in the last pair of pictures has struck the piston corer. Note the changes in orientation and vertical deviation of the piston corer during penetration, pull-out, and ascent - in this case these changes were not extreme.

1.8m (6ft.)
FOCUS



4.9m (16ft.)
FOCUS

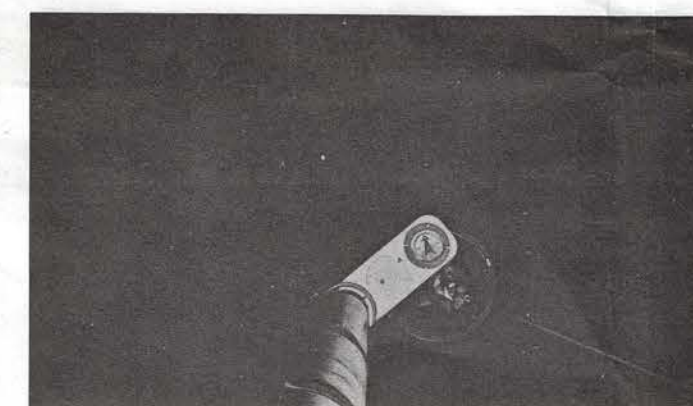


TIME
INTERVAL

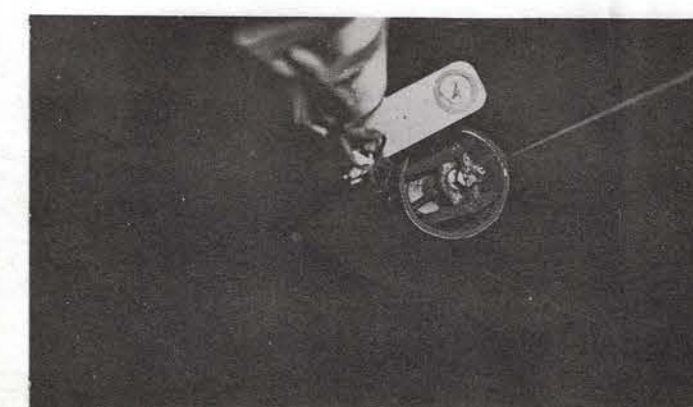
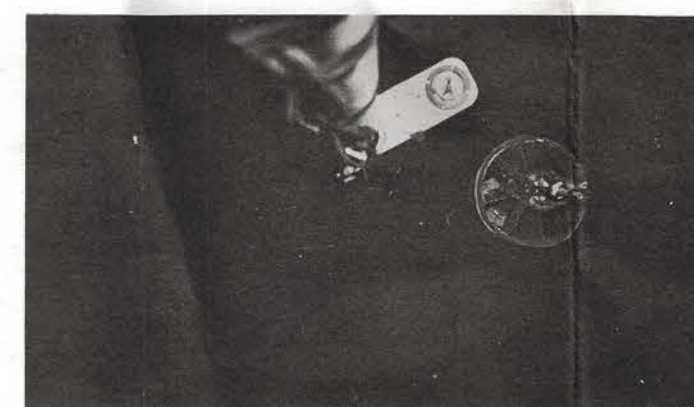
PENETRATION

BOTTOM

1.8m (6ft.)
FOCUS



4.9m (16ft.)
FOCUS



TIME
INTERVAL

PULL-OUT

ASCENT

Plate I. Sequence of photographs taken by both cameras during coring operations on station 7.

DISTRIBUTION LIST 4029

Office of Naval Research		Director	
Department of the Navy		Naval Research Laboratory	2
Attn: Code 480	1	Attn: Code 2021	
480 D	1	Washington, D.C. 20390	
460	1		
466	5	Commander	
468	1	Naval Oceanographic Office	2
414	1	Washington, D.C. 20390	
Washington, D. C. 20360			
Chief of Naval Operations		Chief Scientist	1
Department of the Navy		Naval Research Laboratory	
Attn: OP 07	1	Underwater Sound Reference Div.	
71	1	P.O. Box 8337	
95	1	Orlando, Florida 32806	
Washington, D. C. 20350			
Director		Commanding Officer and Director	
Office of Naval Research	1	Navy Electronics Laboratory	
Branch Office		Attn: Code 3060C	1
495 Summer Street		Code 3102	1
Boston, Massachusetts 02210		San Diego, California 92152	
Director		Commanding Officer	
Office of Naval Research	1	Naval Ordnance Laboratory	1
Branch Office		White Oak, Maryland 20910	
New York Area Office			
207 West 24th Street		Commanding Officer and Director	
New York, New York 10011		Naval Underwater Weapons Research	1
		and Engineering Station	
		Newport, Rhode Island 02844	
Commander		Commanding Officer and Director	1
Naval Ship Systems Command		Naval Civil Engineering Laboratory	
Department of the Navy		Port Hueneme, California 93401	
Attn: SHIPS 03	1		
1622C1	1	Commanding Officer	
Washington, D.C. 20360		Navy Air Development Center	1
		Attn: NADC Library	
		Johnsville, Pennsylvania 18974	
Commander			
Naval Air Systems Command	1	Superintendent	
Department of the Navy		U.S. Naval Academy	
Attn: AIR 370E		Annapolis, Maryland 21402	
Washington, D.C. 20360			
Chief of Naval Material	1	Office of Naval Research	
Department of the Navy		Project Officer	1
Attn: DCNM/DND (Development)		U.S. Sofar Station	
Washington, D.C. 20360		APO 856	
		New York, New York 09856	
Assistant Secretary of the Navy	1		
For Research and Development			
Department of the Navy			
Washington D.C.			

Commanding Officer and Director Naval Underwater Sound Laboratory Fort Trumbull New London, Connecticut 06321	1	Mr. Theodore V. Ryan Director Pacific Oceanographic Research Laboratory 1801 Fairview Avenue East Seattle, Washington 98102	1
Commanding Officer and Director Navy Mine Defense Laboratory Panama City, Florida 32402	1	Commander Naval Ordnance Test Station Attn: Technical Library China Lake, California 93557	1
Office Chief of Research and Development Department of the Army Washington, D.C. 20310	1	Naval Ordnance Test Station Pasadena Annex 3202 East Foothill Blvd. Attn: Library Pasadena, California 91107	1
U.S. Army Beach Erosion Board 5201 Little Falls Rd., N.W. Washington, D.C. 20016	1	Naval Post Graduate School Attn: Librarian Dept. of Meteorology and Oceanography Monterey, California 93940	1 2
Defense Documentation Center Cameron Station Alexandria, Virginia 22314	20	Naval Applied Science Laboratory Naval Base Attn: Technical Library Code 222 Brooklyn, New York 11251	1
National Academy of Sciences National Research Council 2101 Constitution Ave., N.W. Attn: Committee on Undersea Warfare Committee on Oceanography Washington, D.C. 20418	1 1	Advanced Research Projects Agencies Attn: Nuclear Test Detection Office Washington, D.C. 20301	1
ESSA U.S. Department of Commerce Attn: Institute of Oceanography Institute of Atmospheric Sciences Washington, D.C. 20235	1 1	Director Scripps Institution of Oceanography La Jolla, California 92083	1
Geological Division Marine Geology Unit U.S. Geological Survey Washington, D.C. 20240	1	Ordnance Research Laboratory Pennsylvania State University University Park, Penn. 16801	1
U.S. Geological Survey Marine Geology and Hydrology 345 Middlefield Road Attn: Dr. Rusnak Menlo Park, California 94025	1	Director Marine Physical Laboratory Scripps Institution of Oceanography San Diego, California 92152	1
Director Oceanography Museum of Natural History Smithsonian Institution Washington, D.C. 20560	1	Director Marine Laboratory University of Miami #1 Rickenbacker Causeway Miami, Florida 33194	1

Director
Department of Oceanography
and Meteorology 1
Texas A & M University
College Station, Texas 77843

Hawaii Technical Information Center
567 South King Street
Honolulu, Hawaii 96813 1

Head, Department of Oceanography 1
Oregon State University
Corvallis, Oregon 97331

National Institute of Oceanography
Wormley, Godalming
Surrey, England
Attn: Librarian 1

Director
Arctic Research Laboratory 1
Point Barrow, Alaska 99723

Head, Department of Oceanography
University of Washington 1
Seattle, Washington 98105

Geophysical Institute of the
University of Alaska 1
College, Alaska 99735

Applied Physics Laboratory
University of Washington 1
1013 NE Fortieth Street
Seattle, Washington 98105

Department of Geodesy and
Geophysics 1
Cambridge University
Cambridge, England

Director
Institute of Geophysics 1
University of Hawaii
Honolulu, Hawaii 96825

Director
Applied Research Laboratories 1
University of Texas
Austin, Texas 78712

Bell Telephone Laboratories, Inc.
Attn: Mr. E.E. Sumner, Div. 54
Whippany, New Jersey 07981 1

U.S. Naval Schools, Mine Warfare
U.S. Naval Base 1
Charleston, South Carolina 29408

Woods Hole Oceanographic Institution
Reference No. 69-19

DEEP-SEA COREHEAD CAMERA PHOTOGRAPHY AND PISTON CORING by F. W. McCoy, Jr., R. P. Von Herzen, U. H. Owen and P. R. Boutin. 66 pages. March 1969. Contract Nonr-4029(00); NR 260-101, N00014-66-C0241; HR 083-004; and with National Science Foundation Grants GA-1077 and GA-1209.

Cameras mounted in a corehead of a piston corer were used to photograph coring operations during 36 stations on CHAIN cruise 75 and 28 stations on ATLANTIS II cruise 42. The deep-water operation of a piston corer during its descent, tripping, impact with the bottom, and ascent has been studied, providing information on the corer's stability, effectiveness and influence on the nearby sea-floor. Photographic determinations of the amount of penetration allowed comparisons with more indirect methods of determining penetration and with core recovery. Sediment clouds produced by coring were studied for bottom currents.

The corer descends with little rotation and swinging. Free-fall and penetration generally take place in less than 5 seconds, with a rotation of 20-60° and an increase of about 6° in vertical deviation. The coring process produces mounds and depressions around the core barrels. While resting in the bottom, the corer is stable except for occasional wobbling. Considerable rotation takes place during both pull-out and ascent with frequent sediment discharges from the corer. No consistent relationship was found between the amount of penetration and the length of core recovered. Comparisons indicate that the piston cores have been shortened and disturbed relative to the pilot cores, and that as much as a meter of the upper portion of the piston core has been lost. The position of the mud-mark appears to be a reliable indicator of the amount of penetration; estimates by extrapolation of the thermal gradient to the surface are less reliable. The vertical deviation of the corer in the bottom does not influence the amount of penetration. Stratigraph dips in the recovered cores correspond poorly to this vertical deviation in the bottom.

1. Coring photography
 2. Deep-sea photography
 3. Piston Coring
- I. McCoy, F. W., Jr.
 - II. Von Herzen, R. P.
 - III. Owen, U. H.
 - IV. Boutin, P. R.
 - V. Nonr-4029(00); NR 260-101
 - VI. N00014-66-C0241; NR 083-004
 - VII. GA-1077 and GA-1209

This card is UNCLASSIFIED

Woods Hole Oceanographic Institution
Reference No. 69-19

DEEP-SEA COREHEAD CAMERA PHOTOGRAPHY AND PISTON CORING by F. W. McCoy, Jr., R. P. Von Herzen, U. H. Owen and P. R. Boutin. 66 pages. March 1969. Contract Nonr-4029(00); NR 260-101, N00014-66-C0241; HR 083-004; and with National Science Foundation Grants GA-1077 and GA-1209.

Cameras mounted in a corehead of a piston corer were used to photograph coring operations during 36 stations on CHAIN cruise 75 and 28 stations on ATLANTIS II cruise 42. The deep-water operation of a piston corer during its descent, tripping, impact with the bottom, and ascent has been studied, providing information on the corer's stability, effectiveness and influence on the nearby sea-floor. Photographic determinations of the amount of penetration allowed comparisons with more indirect methods of determining penetration and with core recovery. Sediment clouds produced by coring were studied for bottom currents.

The corer descends with little rotation and swinging. Free-fall and penetration generally take place in less than 5 seconds, with a rotation of 20-60° and an increase of about 6° in vertical deviation. The coring process produces mounds and depressions around the core barrels. While resting in the bottom, the corer is stable except for occasional wobbling. Considerable rotation takes place during both pull-out and ascent with frequent sediment discharges from the corer. No consistent relationship was found between the amount of penetration and the length of core recovered. Comparisons indicate that the piston cores have been shortened and disturbed relative to the pilot cores, and that as much as a meter of the upper portion of the piston core has been lost. The position of the mud-mark appears to be a reliable indicator of the amount of penetration; estimates by extrapolation of the thermal gradient to the surface are less reliable. The vertical deviation of the corer in the bottom does not influence the amount of penetration. Stratigraph dips in the recovered cores correspond poorly to this vertical deviation in the bottom.

1. Coring photography
 2. Deep-sea photography
 3. Piston Coring
- I. McCoy, F. W., Jr.
 - II. Von Herzen, R. P.
 - III. Owen, U. H.
 - IV. Boutin, P. R.
 - V. Nonr-4029(00); NR 260-101
 - VI. N00014-66-C0241; NR 083-004
 - VII. GA-1077 and GA-1209

This card is UNCLASSIFIED

Woods Hole Oceanographic Institution
Reference No. 69-19

DEEP-SEA COREHEAD CAMERA PHOTOGRAPHY AND PISTON CORING by F. W. McCoy, Jr., R. P. Von Herzen, U. H. Owen and P. R. Boutin. 66 pages. March 1969. Contract Nonr-4029(00); NR 260-101, N00014-66-C0241; HR 083-004; and with National Science Foundation Grants GA-1077 and GA-1209.

Cameras mounted in a corehead of a piston corer were used to photograph coring operations during 36 stations on CHAIN cruise 75 and 28 stations on ATLANTIS II cruise 42. The deep-water operation of a piston corer during its descent, tripping, impact with the bottom, and ascent has been studied, providing information on the corer's stability, effectiveness and influence on the nearby sea-floor. Photographic determinations of the amount of penetration allowed comparisons with more indirect methods of determining penetration and with core recovery. Sediment clouds produced by coring were studied for bottom currents.

The corer descends with little rotation and swinging. Free-fall and penetration generally take place in less than 5 seconds, with a rotation of 20-60° and an increase of about 6° in vertical deviation. The coring process produces mounds and depressions around the core barrels. While resting in the bottom, the corer is stable except for occasional wobbling. Considerable rotation takes place during both pull-out and ascent with frequent sediment discharges from the corer. No consistent relationship was found between the amount of penetration and the length of core recovered. Comparisons indicate that the piston cores have been shortened and disturbed relative to the pilot cores, and that as much as a meter of the upper portion of the piston core has been lost. The position of the mud-mark appears to be a reliable indicator of the amount of penetration; estimates by extrapolation of the thermal gradient to the surface are less reliable. The vertical deviation of the corer in the bottom does not influence the amount of penetration. Stratigraph dips in the recovered cores correspond poorly to this vertical deviation in the bottom.

1. Coring photography
 2. Deep-sea photography
 3. Piston Coring
- I. McCoy, F. W., Jr.
 - II. Von Herzen, R. P.
 - III. Owen, U. H.
 - IV. Boutin, P. R.
 - V. Nonr-4029(00); NR 260-101
 - VI. N00014-66-C0241; NR 083-004
 - VII. GA-1077 and GA-1209

This card is UNCLASSIFIED

Woods Hole Oceanographic Institution
Reference No. 69-19

DEEP-SEA COREHEAD CAMERA PHOTOGRAPHY AND PISTON CORING by F. W. McCoy, Jr., R. P. Von Herzen, U. H. Owen and P. R. Boutin. 66 pages. March 1969. Contract Nonr-4029(00); NR 260-101, N00014-66-C0241; HR 083-004; and with National Science Foundation Grants GA-1077 and GA-1209.

Cameras mounted in a corehead of a piston corer were used to photograph coring operations during 36 stations on CHAIN cruise 75 and 28 stations on ATLANTIS II cruise 42. The deep-water operation of a piston corer during its descent, tripping, impact with the bottom, and ascent has been studied, providing information on the corer's stability, effectiveness and influence on the nearby sea-floor. Photographic determinations of the amount of penetration allowed comparisons with more indirect methods of determining penetration and with core recovery. Sediment clouds produced by coring were studied for bottom currents.

The corer descends with little rotation and swinging. Free-fall and penetration generally take place in less than 5 seconds, with a rotation of 20-60° and an increase of about 6° in vertical deviation. The coring process produces mounds and depressions around the core barrels. While resting in the bottom, the corer is stable except for occasional wobbling. Considerable rotation takes place during both pull-out and ascent with frequent sediment discharges from the corer. No consistent relationship was found between the amount of penetration and the length of core recovered. Comparisons indicate that the piston cores have been shortened and disturbed relative to the pilot cores, and that as much as a meter of the upper portion of the piston core has been lost. The position of the mud-mark appears to be a reliable indicator of the amount of penetration; estimates by extrapolation of the thermal gradient to the surface are less reliable. The vertical deviation of the corer in the bottom does not influence the amount of penetration. Stratigraph dips in the recovered cores correspond poorly to this vertical deviation in the bottom.

1. Coring photography
 2. Deep-sea photography
 3. Piston Coring
- I. McCoy, F. W., Jr.
 - II. Von Herzen, R. P.
 - III. Owen, U. H.
 - IV. Boutin, P. R.
 - V. Nonr-4029(00); NR 260-101
 - VI. N00014-66-C0241; NR 083-004
 - VII. GA-1077 and GA-1209

This card is UNCLASSIFIED

UNCLASSIFIED

Security Classification

DOCUMENT CONTROL DATA - R&D

(Security classification of title, body of abstract and indexing annotation must be entered when the overall report is classified)

1. ORIGINATING ACTIVITY <i>(Corporate author)</i> Woods Hole Oceanographic Institution Woods Hole, Massachusetts	2a. REPORT SECURITY CLASSIFICATION Unclassified
	2b. GROUP

3. REPORT TITLE
DEEP-SEA COREHEAD CAMERA PHOTOGRAPHY AND PISTON CORING

4. DESCRIPTIVE NOTES *(Type of report and inclusive dates)*
Technical Report

5. AUTHOR(S) *(Last name, first name, initial)*
McCoy, F. W., Jr., Von Herzen, R. P., Owen, D. M., Boutin, P. R.

6. REPORT DATE March 1969	7a. TOTAL NO. OF PAGES 66	7b. NO. OF REFS
-------------------------------------	-------------------------------------	-----------------

8a. CONTRACT OR GRANT NO. Nonr-4029(00); NR 260-101, b. PROJECT NO. N00014-66-C0241; NR 083-004 GA-1077 and GA-1209 c. d.	9a. ORIGINATOR'S REPORT NUMBER(S) WHOI Reference No. 69-19
	9b. OTHER REPORT NO(S) <i>(Any other numbers that may be assigned this report)</i>

10. AVAILABILITY/LIMITATION NOTICES
This document has been approved for public release and sale; its distribution is unlimited.

11. SUPPLEMENTARY NOTES	12. SPONSORING MILITARY ACTIVITY Office of Naval Research Washington, D.C.
-------------------------	--

13. ABSTRACT
SEE LIBRARY CARD

14. KEY WORDS	LINK A		LINK B		LINK C	
	ROLE	WT	ROLE	WT	ROLE	WT
1. Coring photography						
2. Deep-sea photography						
3. Piston Coring						

INSTRUCTIONS

1. **ORIGINATING ACTIVITY:** Enter the name and address of the contractor, subcontractor, grantee, Department of Defense activity or other organization (*corporate author*) issuing the report.
- 2a. **REPORT SECURITY CLASSIFICATION:** Enter the overall security classification of the report. Indicate whether "Restricted Data" is included. Marking is to be in accordance with appropriate security regulations.
- 2b. **GROUP:** Automatic downgrading is specified in DoD Directive 5200.10 and Armed Forces Industrial Manual. Enter the group number. Also, when applicable, show that optional markings have been used for Group 3 and Group 4 as authorized.
3. **REPORT TITLE:** Enter the complete report title in all capital letters. Titles in all cases should be unclassified. If a meaningful title cannot be selected without classification, show title classification in all capitals in parenthesis immediately following the title.
4. **DESCRIPTIVE NOTES:** If appropriate, enter the type of report, e.g., interim, progress, summary, annual, or final. Give the inclusive dates when a specific reporting period is covered.
5. **AUTHOR(S):** Enter the name(s) of author(s) as shown on or in the report. Enter last name, first name, middle initial. If military, show rank and branch of service. The name of the principal author is an absolute minimum requirement.
6. **REPORT DATE:** Enter the date of the report as day, month, year; or month, year. If more than one date appears on the report, use date of publication.
- 7a. **TOTAL NUMBER OF PAGES:** The total page count should follow normal pagination procedures, i.e., enter the number of pages containing information.
- 7b. **NUMBER OF REFERENCES:** Enter the total number of references cited in the report.
- 8a. **CONTRACT OR GRANT NUMBER:** If appropriate, enter the applicable number of the contract or grant under which the report was written.
- 8b, 8c, & 8d. **PROJECT NUMBER:** Enter the appropriate military department identification, such as project number, subproject number, system numbers, task number, etc.
- 9a. **ORIGINATOR'S REPORT NUMBER(S):** Enter the official report number by which the document will be identified and controlled by the originating activity. This number must be unique to this report.
- 9b. **OTHER REPORT NUMBER(S):** If the report has been assigned any other report numbers (*either by the originator or by the sponsor*), also enter this number(s).
10. **AVAILABILITY/LIMITATION NOTICES:** Enter any limitations on further dissemination of the report, other than those

imposed by security classification, using standard statements such as:

- (1) "Qualified requesters may obtain copies of this report from DDC."
- (2) "Foreign announcement and dissemination of this report by DDC is not authorized."
- (3) "U. S. Government agencies may obtain copies of this report directly from DDC. Other qualified DDC users shall request through _____."
- (4) "U. S. military agencies may obtain copies of this report directly from DDC. Other qualified users shall request through _____."
- (5) "All distribution of this report is controlled. Qualified DDC users shall request through _____."

If the report has been furnished to the Office of Technical Services, Department of Commerce, for sale to the public, indicate this fact and enter the price, if known.

11. **SUPPLEMENTARY NOTES:** Use for additional explanatory notes.
12. **SPONSORING MILITARY ACTIVITY:** Enter the name of the departmental project office or laboratory sponsoring (*paying for*) the research and development. Include address.
13. **ABSTRACT:** Enter an abstract giving a brief and factual summary of the document indicative of the report, even though it may also appear elsewhere in the body of the technical report. If additional space is required, a continuation sheet shall be attached.

It is highly desirable that the abstract of classified reports be unclassified. Each paragraph of the abstract shall end with an indication of the military security classification of the information in the paragraph, represented as (TS), (S), (C), or (U).

There is no limitation on the length of the abstract. However, the suggested length is from 150 to 225 words.

14. **KEY WORDS:** Key words are technically meaningful terms or short phrases that characterize a report and may be used as index entries for cataloging the report. Key words must be selected so that no security classification is required. Identifiers, such as equipment model designation, trade name, military project code name, geographic location, may be used as key words but will be followed by an indication of technical context. The assignment of links, roles, and weights is optional.

